

Coin Sampling: Gradient-Based Bayesian Inference without Learning Rates

Louis Sharrock¹ Christopher Nemeth¹

Abstract

In recent years, particle-based variational inference (ParVI) methods such as Stein variational gradient descent (SVGD) have grown in popularity as scalable methods for Bayesian inference. Unfortunately, the properties of such methods invariably depend on hyperparameters such as the learning rate, which must be carefully tuned by the practitioner in order to ensure convergence to the target measure at a suitable rate. In this paper, we introduce a suite of new particle-based methods for scalable Bayesian inference based on coin betting, which are entirely learning-rate free. We illustrate the performance of our approach on a range of numerical examples, including several high-dimensional models and datasets, demonstrating comparable performance to other ParVI algorithms.

1. Introduction

The task of sampling from complex, high-dimensional probability distributions is of fundamental importance to Bayesian inference (Robert & Casella, 2004; Gelman et al., 2013), machine learning (Neal, 1996; Andrieu et al., 2003; Welling & Teh, 2011; Wilson & Izmailov, 2020), molecular dynamics (Krauth, 2006; Lelièvre & Stoltz, 2016; Leimkuhler & Matthews, 2016), and scientific computing (MacKay, 2003; Liu, 2009). In this paper, we consider the canonical task of sampling from a probability distribution $\pi(dx)$ on \mathbb{R}^d with density $\pi(x)$ with respect to the Lebesgue measure of the form¹

$$\pi(x) := \frac{\exp(-U(x))}{Z} \quad (1)$$

where $U : \mathbb{R}^d \rightarrow \mathbb{R}$ is a measurable, continuously differentiable function known as the potential, and $Z = \int_{\mathbb{R}^d} \exp(-U(x))dx$ is an unknown normalising constant.

¹Department of Mathematics, Lancaster University, UK. Correspondence to: Louis Sharrock <l.sharrock@lancaster.ac.uk>.

¹In a slight abuse of notation, we use π to denote both the measure and its density.

Recently, there has been growing interest in hybrid methods which combine the non-parametric nature of Markov chain Monte Carlo (MCMC) sampling with parameteric approximations using optimisation-based variational inference (VI). In particular, particle based variational inference (ParVI) methods (Liu & Wang, 2016; Chen et al., 2018a; Liu et al., 2019a; Chewi et al., 2020; Korba et al., 2021) approximate the target distribution using an ensemble of interacting particles, which are deterministically updated by minimising the Kullback-Leibler (KL) divergence.

Perhaps the most well known of these methods is Stein variational gradient descent (SVGD). This algorithm iteratively updates the particles according to a form of gradient descent on the KL divergence, with the descent direction restricted to belong to a unit ball in a reproducing kernel Hilbert space (RKHS) (Liu & Wang, 2016). This approach has since given rise to several variants (Liu, 2017; Han & Liu, 2018; Liu & Zhu, 2018; Zhuo et al., 2018; Chen et al., 2018b; Detommaso et al., 2018; Futami et al., 2019a;b; Wang et al., 2019; Chen & Ghattas, 2020; Ye et al., 2020; Liu et al., 2022; Sun & Richtárik, 2022); and found success in a range of problems, including uncertainty quantification (Zhu & Zabaras, 2018), reinforcement learning (Haarnoja et al., 2017; Liu et al., 2017; Zhang et al., 2018), learning deep probabilistic models (Pu et al., 2017; Wang & Liu, 2017), and Bayesian meta-learning (Feng et al., 2017; Yoon et al., 2018).

In order to construct and analyse sampling algorithms of this type, one popular approach is to reformulate the sampling problem as an optimisation problem in the space of measures (Jordan et al., 1998; Liu, 2017; Wibisono, 2018; Cheng & Bartlett, 2018; Durmus et al., 2019). In this setting, one views the target π as the solution of an optimisation problem

$$\pi = \arg \min_{\mu \in \mathcal{P}_2(\mathbb{R}^d)} \mathcal{F}(\mu), \quad (2)$$

where $\mathcal{P}_2(\mathbb{R}^d)$ denotes the set of probability measures $\{\mu : \int_{\mathbb{R}^d} \|x\|^2 \mu(dx) < \infty\}$, and $\mathcal{F} : \mathcal{P}(\mathbb{R}^d) \rightarrow \mathbb{R}$ is a functional which is uniquely minimised at π . A general strategy for solving this problem is then to simulate a time-discretisation of the gradient flow of \mathcal{F} over $\mathcal{P}_2(\mathbb{R}^d)$, having equipped this space with a suitable metric (Ambrosio et al., 2008).

Many popular sampling algorithms can be understood from this perspective. For example, Langevin Monte Carlo (LMC), a popular MCMC algorithm, corresponds to the

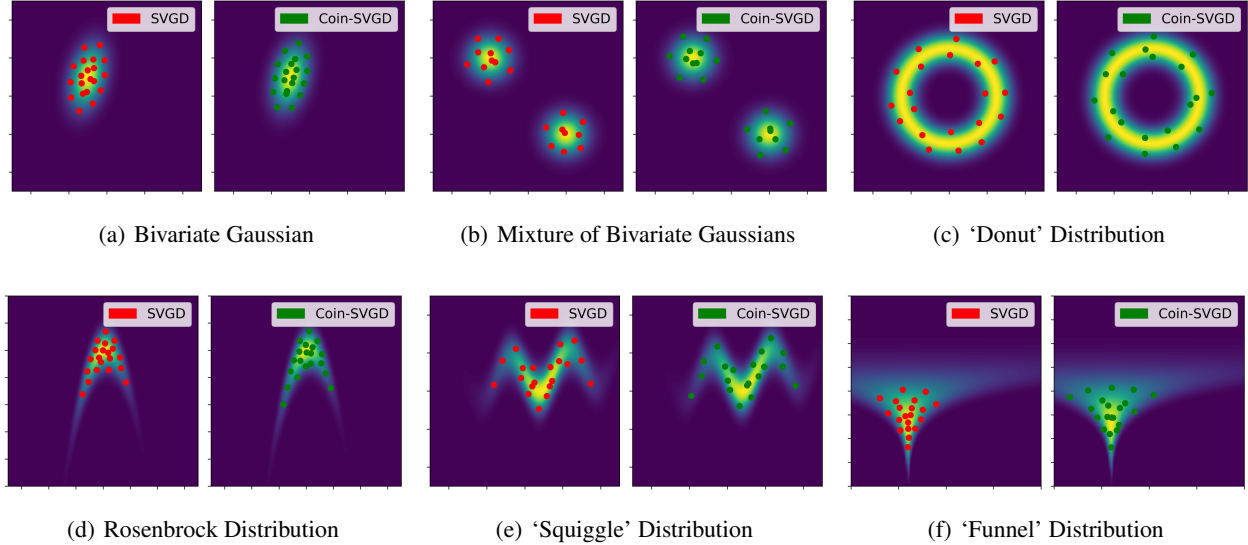


Figure 1. A comparison between SVGD (Liu & Wang, 2016) and its learning-rate free analogue, Coin SVGD (Algorithm 2). We plot the samples generated by both methods for several two-dimensional target distributions. Further details are provided in Section 4.1 and Appendix E.1.

so-called forward-flow discretisation of the gradient flow of the KL divergence with respect to the quadratic Wasserstein metric (Wibisono, 2018; Durmus et al., 2019).² Meanwhile, SVGD can be viewed as the explicit Euler discretisation of the gradient flow of the KL divergence with respect to a kernelised Wasserstein metric (Liu, 2017; Duncan et al., 2019). Other more recent examples, designed with this perspective in mind, include maximum mean discrepancy (MMD) gradient descent (Arbel et al., 2019), the Wasserstein proximal gradient algorithm (Salim et al., 2020), kernel Stein discrepancy descent (KSDD) (Korba et al., 2021), Laplacian adjusted Wasserstein gradient descent (LAWGD) (Chewi et al., 2020), mollified energy interaction descent (MEID) (Li et al., 2022), and the various other ParVI methods described in (Chen et al., 2018a; Liu et al., 2019a;b).

One feature common to all of these approaches is the need to specify an appropriate learning rate (i.e., step size) γ , or a learning rate schedule $(\gamma_t)_{t \geq 1}$. This learning rate must be sufficiently small to ensure convergence to the target measure, or a close approximation thereof, but also large enough to ensure convergence within a reasonable time period. In theory, for a given target π , existing non-asymptotic convergence rates allow one to derive an optimal learning rate (see, e.g., Korba et al., 2020; Salim et al., 2022; Sun & Richtárik, 2022 for SVGD; Dalalyan, 2017a;b; Durmus & Moulines, 2017; Dalalyan & Karagulyan, 2019; Durmus & Moulines,

2019 for LMC). Invariably, however, the optimal learning rate is a function of the unknown target measure (e.g., Corollary 6 in Korba et al., 2020; Theorem 9 in Durmus et al., 2019) and thus, in practice, cannot be computed.

With these considerations in mind, a natural question is whether one can obtain a gradient-based sampling method which does not require a learning rate. In this paper, we answer this question in the affirmative. In particular, inspired by the parameter-free optimisation methods developed by Orabona and coworkers (Orabona, 2014; Orabona & Pal, 2016; Orabona & Tommasi, 2017; Cutkosky & Orabona, 2018; Jun & Orabona, 2019; Chen et al., 2022a), and leveraging the view of sampling as an optimisation problem in the space of measures (Wibisono, 2018), we obtain a new suite of particle-based algorithms for scalable Bayesian inference which are entirely learning rate free. Similar to other ParVIs, our algorithms deterministically update an ensemble of interacting particles in order to approximate the target distribution. However, unlike other ParVIs, our algorithms do not correspond to the time-discretisation of any gradient flow, and thus bear little resemblance to existing methods.

Under the assumption of log-concavity, we outline how to establish convergence to the target measure in the infinite-particle regime, and how to obtain a non-asymptotic convergence rate. We then illustrate the performance of our approach on a range of numerical examples, including both convex and non-convex targets. Our results indicate that the proposed methodology achieves comparable performance to existing particle-based sampling algorithms in a range of tasks, with no need to tune a learning rate.

²The connection between the law of the overdamped Langevin diffusion (i.e., the continuous-time dynamics of LMC) and the gradient flow of the KL divergence dates back to Otto et al. (Jordan et al., 1998; Otto, 2001; Otto & Westdickenberg, 2005).

2. Preliminaries

2.1. Optimisation in Euclidean Space

We begin by reviewing optimisation in Euclidean spaces, focusing on the learning-rate free stochastic optimisation method introduced by [Orabona & Pal \(2016\)](#). This will later provide the foundation for our learning-rate free sampling method.

2.1.1. NOTATION

Let $\mathcal{X} \subseteq \mathbb{R}^d$, and write $\|\cdot\|$ and $\langle \cdot, \cdot \rangle$ for the Euclidean norm and inner product in \mathbb{R}^d . Let $f : \mathcal{X} \rightarrow \mathbb{R} \cup \{-\infty, \infty\}$, and let $f^* : \mathcal{X}^* \rightarrow \mathbb{R} \cup \{-\infty, \infty\}$ denote the Fenchel conjugate of f , so that $f^*(u) = \sup_{x \in \mathcal{X}} [\langle u, x \rangle - f(x)]$.

Suppose that f is m -strongly convex, for some $m \geq 0$. Let $x \in \mathcal{X}$. We say that $g \in \mathcal{X}$ is a subgradient of f at x , and write $g \in \partial f(x)$ if, for any $z \in \mathcal{X}$,

$$f(z) - f(x) \geq \langle g, z - x \rangle + \frac{m}{2} \|z - x\|^2 \quad (3)$$

If f is differentiable at x , then the differential set $\partial f(x)$ contains a single element, $\partial f(x) = \{\nabla f(x)\}$, where $\nabla f(x)$ denotes the gradient of f at x .

2.1.2. EUCLIDEAN GRADIENT FLOWS

Suppose we are interested in the optimisation problem

$$x^* = \arg \min_{x \in \mathcal{X}} f(x), \quad (4)$$

where $f : \mathcal{X} \rightarrow \mathbb{R}$ is m -strongly convex. We can solve this problem using the gradient flow of f , defined as the solution $x : [0, \infty) \rightarrow \mathbb{R}^d$ of the following differential inclusion

$$\dot{x}_t \in -\partial f(x_t), \quad (5)$$

with initial condition $x_0 = x_{\text{init}}$. This inclusion admits a unique, absolutely continuous solution for almost all $t \geq 0$ (e.g., Theorem 3.1 in [Brézis, 1973](#), Theorem 2.7 in [Peypouquet & Sorin, 2010](#); Proposition 2.1 in [Santambrogio, 2017](#)). Moreover, the function $t \mapsto f(x_t)$ is decreasing, with $\lim_{t \rightarrow \infty} f(x_t) = \inf_{x \in \mathcal{X}} f(x)$ ([Peypouquet & Sorin, 2010](#), Proposition 3.1).

In practice, it is necessary to use a time-discretisation of this gradient flow. One standard choice is a backward Euler discretisation, which results in the proximal point algorithm ([Güler, 1991](#); [De Giorgi, 1993](#)). Alternatively, one can utilise a forward Euler discretisation, which results in the standard subgradient descent algorithm ([Shor, 1985](#))

$$x_{t+1} = x_t + \gamma \nabla g_t, \quad g_t \in \partial f(x_t). \quad (6)$$

The properties of this algorithm depend, necessarily, on the choice of learning rate $\gamma > 0$. For example, given

an L -Lipschitz function, it is well known that the average of the algorithm iterates $\bar{x}_T = \frac{1}{T} \sum_{t=1}^T x_t$ satisfies (e.g., [Zinkevich, 2003](#))

$$f(\bar{x}_T) - f(x^*) \leq \frac{1}{T} \left[\frac{\|x_1 - x^*\|^2}{2\gamma} + \frac{L^2 T \gamma}{2} \right]. \quad (7)$$

Using this expression, one can obtain the ‘ideal’ learning rate as $\gamma_{\text{ideal}} = \frac{\|x_1 - x^*\|}{L\sqrt{T}}$, which implies the optimal error bound

$$f(\bar{x}_T) - f(x^*) \leq \frac{L\|x_1 - x^*\|}{\sqrt{T}}. \quad (8)$$

In practice, however, it is not possible to achieve this bound. Indeed, even in hindsight, one cannot compute the ideal learning rate γ_{ideal} , since it depends on the unknown $\|x_1 - x^*\|$.

2.1.3. LEARNING-RATE FREE GRADIENT DESCENT

Following [Orabona & Pal \(2016\)](#), we now outline an alternative approach for solving the stochastic optimisation problem in (4) which is entirely learning-rate free. Consider a gambler who bets on the outcomes of a series of adversarial coin flips. Suppose that the gambler starts with an initial wealth $w_0 = \varepsilon > 0$. In the t^{th} round, the gambler bets on the outcome of a coin flip $c_t \in \{-1, 1\}$, where $+1$ denotes heads and -1 denotes tails. For now, we make no assumptions on how c_t is generated.

We will encode the gambler’s bet in the t^{th} round by $x_t \in \mathbb{R}$. In particular, $\text{sign}(x_t) \in \{-1, 1\}$ will denote whether the bet is on heads or tails, and $|x_t| \in \mathbb{R}$ will denote the size of the bet. Thus, in the t^{th} round, the gambler wins $x_t c_t$ if $\text{sign}(c_t) = \text{sign}(x_t)$; and loses $x_t c_t$ otherwise. Finally, we will write w_t for the wealth of the gambler at the end of the t^{th} round. Clearly, we then have that

$$w_t = \varepsilon + \sum_{i=1}^t c_i x_i. \quad (9)$$

We will restrict our attention to the case in which the gambler’s bets satisfy $x_t = \beta_t w_{t-1}$, for some betting fraction $\beta_t \in [-1, 1]$. This is equivalent to the assumption that the gambler cannot borrow any money.

We will now outline how to solve the convex optimisation problem $x^* = \arg \min_{x \in \mathbb{R}} f(x)$ using a coin-betting algorithm. For simplicity, we will restrict our attention to the simple one-dimensional function $f(x) = |x - 10|$. We note, however, that this approach can easily be extended to any convex function $f : \mathbb{R}^d \rightarrow \mathbb{R}$ ([Orabona & Pal, 2016](#)). Suppose we define the outcome of a coin flip $c_t \in \{-1, 1\}$ to be equal to $-g_t \in \partial[-f(x_t)]$, the negative subgradient of $f(x_t)$. In this case, under a certain assumption on the betting strategy $(\beta_t)_{t=1}^T$, [Orabona & Pal \(2016\)](#) show that the average of bets $f(\bar{x}_T)$ converges to $f(x^*)$, with a rate which depends on the quality of the betting strategy.

Lemma 2.1. *Suppose that the betting strategy $(\beta_t)_{t=1}^T$ guarantees that, for any sequence of coin flips $(c_t)_{t=1}^T \in [-1, 1]$, there exists a function $h : \mathbb{R} \rightarrow \mathbb{R}$ such that the wealth after T rounds satisfies $w_T \geq h(\sum_{t=1}^T c_t)$. Then*

$$f\left(\frac{1}{T} \sum_{t=1}^T x_t\right) - f(x^*) \leq \frac{h^*(x^*) + \varepsilon}{T} \quad (10)$$

Proof. See Appendix B. \square

We can thus use any suitable coin-betting algorithm to obtain $x^* = \arg \min_{x \in \mathbb{R}} f(x)$, given access to the subgradients of f . Any such algorithm will be entirely learning-rate free. There are various betting strategies which satisfy the inequality $w_T \geq h(\sum_{t=1}^T c_t)$ (e.g., [Orabona & Pal, 2016](#); [Orabona & Tommasi, 2017](#); [Chen et al., 2022a](#)). Perhaps the simplest such strategy is one based on the Krichevsky-Trofimov (KT) estimator ([Krichevsky & Trofimov, 1981](#)), which defines the betting strategy to be equal to $\beta_t = \sum_{i=1}^{t-1} c_i/t$. This results in the coin betting algorithm

$$x_t = -\frac{\sum_{i=1}^{t-1} g_i}{t} \left(\varepsilon - \sum_{i=1}^{t-1} g_i x_i \right). \quad (11)$$

In this case, it is possible to show ([Orabona & Pal, 2016](#), Lemma 14) that the wealth is lower bounded by

$$h\left(\sum_{t=1}^T c_t\right) = \frac{\varepsilon}{K\sqrt{T}} \exp\left(\frac{\left(\sum_{t=1}^T c_t\right)^2}{2T}\right), \quad (12)$$

where K is a universal constant. Thus, using Lemma 2.1 and an appropriate bound on the convex conjugate of h , one obtains ([Orabona & Pal, 2016](#), Corollary 5)

$$f(\bar{x}_T) - f(x^*) \leq K \frac{\|x^*\| \sqrt{\log(1 + \frac{24T^2 \|x^*\|^2}{\varepsilon^2})} + \varepsilon}{\sqrt{T}}. \quad (13)$$

It is instructive to compare this bound with (8), the corresponding bound for subgradient descent with an optimally chosen learning rate. Although the coin-betting approach does not quite achieve the optimal bound in (8), it comes close, containing only an additional log-factor. This can be viewed as the trade-off for the fact that the algorithm is now learning-rate free.

3. Coin Sampling for Bayesian Inference

Our approach, summarised in Algorithm 1, can be viewed as a natural extension of the learning-rate free optimisation methods introduced in Section 2.1.3 to the Wasserstein space. In particular, coin sampling utilises Wasserstein gradients, approximated via a set of interacting particles, within the coin-betting framework, to obtain a learning-rate free Bayesian inference algorithm.

3.1. Optimisation in Wasserstein Space

To extend coin betting to our setting, we will require some basic concepts from optimal transport, including the definition of the Wasserstein space and Wasserstein gradient flow. We provide additional details on geodesic convexity and subdifferential calculus in Appendix A; see also the books of [Ambrosio et al. \(2008\)](#) and [Villani \(2008\)](#).

3.1.1. THE WASSERSTEIN SPACE

For $p \geq 1$, let $\mathcal{P}_p(\mathbb{R}^d)$ denote the set of probability measures on \mathbb{R}^d with finite p^{th} moment: $\int_{\mathbb{R}^d} \|x\|^p \mu(dx) < \infty$. For any $\mu \in \mathcal{P}_p(\mathbb{R}^d)$, let $L^p(\mu)$ denote the set of measurable functions $f : \mathbb{R}^d \rightarrow \mathbb{R}^d$ such that $\int_{\mathbb{R}^d} \|f(x)\|^p \mu(dx) < \infty$. We will write $\|\cdot\|_{L^2(\mu)}^2$ and $\langle \cdot, \cdot \rangle_{L^2(\mu)}$ to denote, respectively, the norm and the inner product of this space.

Given a probability measure $\mu \in \mathcal{P}_2(\mathbb{R}^d)$ and a measurable function $T : \mathbb{R}^d \rightarrow \mathbb{R}^d$, we write $T_{\#}\mu$ for the pushforward measure of μ under T , that is, the measure such that $T_{\#}\mu(B) = \mu(T^{-1}(B))$ for all Borel measurable $B \in \mathcal{B}(\mathbb{R}^d)$. For every $\mu, \nu \in \mathcal{P}_p(\mathbb{R}^d)$, let $\Gamma(\mu, \nu)$ be the set of couplings (or transport plans) between μ and ν , defined as $\Gamma(\mu, \nu) = \{\gamma \in \mathcal{P}_p(\mathbb{R}^d) : Q_{\#}^1 \gamma = \mu, Q_{\#}^2 \gamma = \nu\}$, where Q^1 and Q^2 denote the projections onto the first and second components of $\mathbb{R}^d \times \mathbb{R}^d$. The Wasserstein p -distance between μ and ν is then defined according to

$$W_p^p(\mu, \nu) = \inf_{\gamma \in \Gamma(\mu, \nu)} \int_{\mathbb{R}^d \times \mathbb{R}^d} \|x - y\|^p \gamma(dx, dy). \quad (14)$$

The Wasserstein distance W_2 is a distance over $\mathcal{P}_2(\mathbb{R}^d)$. Thus $(\mathcal{P}_2(\mathbb{R}^d), W_2)$ is a metric space of probability measures, known as the Wasserstein space. One important property of W_2 is that, under certain regularity conditions, there exists a unique optimal coupling $\gamma_* \in \Gamma(\mu, \nu)$ which minimises the transport cost $\int_{\mathbb{R}^d \times \mathbb{R}^d} \|x - y\|^2 \gamma_*(dx, dy)$. This optimal coupling is of the form $\gamma = (\text{id} \times t_{\mu}^{\nu})_{\#}\mu$, where $\text{id} : \mathbb{R}^d \rightarrow \mathbb{R}^d$ is the identity map, and t_{μ}^{ν} is known as the optimal transport map ([Brenier, 1991](#); [Gigli, 2011](#)). It follows that $(t_{\mu}^{\nu})_{\#}\mu = \nu$ and $W_2^2(\mu, \nu) = \int_{\mathbb{R}^d} \|x - y\|^2 \gamma_*(dx, dy) = \int_{\mathbb{R}^d} \|x - t_{\mu}^{\nu}(x)\|^2 dx$.

3.1.2. WASSERSTEIN GRADIENT FLOWS

Recall the optimisation problem from Section 1,

$$\pi = \arg \min_{\mu \in \mathcal{P}_2(\mathbb{R}^d)} \mathcal{F}(\mu), \quad (15)$$

where $\mathcal{F} : \mathcal{P}_2(\mathbb{R}^d) \rightarrow (-\infty, \infty]$ is a proper, lower semi-continuous functional uniquely minimised at π . There are various possible choices for the functional \mathcal{F} (see, e.g., [Simon-Gabriel, 2018](#)). In the context of Bayesian inference, perhaps the most common choice is $\text{KL}(\mu|\pi)$, the Kullback-Leibler (KL) divergence of μ with respect to π . Other

possibilities include the chi-squared divergence $\mathcal{X}^2(\mu|\pi)$ (Chewi et al., 2020), and the maximum mean discrepancy $\text{MMD}(\mu|\pi)$ (Arbel et al., 2019), of which the kernel Stein discrepancy $\text{KSD}(\mu|\pi)$ (Korba et al., 2021) is a special case.

Similarly to the Euclidean case, typical solutions to (15) are based on the use of a gradient flow. In particular, we now consider the Wasserstein gradient flow of \mathcal{F} , defined as the weak solution $\mu : [0, \infty) \rightarrow \mathcal{P}_2(\mathbb{R}^d)$ of the continuity equation (Ambrosio et al., 2008, Chapter 11)

$$\partial_t \mu_t + \nabla \cdot (v_t \mu_t) = 0, \quad v_t \in -\partial \mathcal{F}(\mu_t). \quad (16)$$

where $\partial \mathcal{F}(\mu)$ denotes the Fréchet subdifferential $\partial \mathcal{F}(\mu)$ of \mathcal{F} at μ (see Appendix A). Under mild conditions, this equation admits a unique solution for any initial condition (e.g., Theorem 11.1.4 and Theorem 11.2.1 in Ambrosio et al., 2008; Proposition 4.13 in Santambrogio, 2017). In addition, the function $t \mapsto \mathcal{F}(\mu_t)$ is decreasing, so that $\lim_{t \rightarrow \infty} \mathcal{F}(\mu_t) = \inf_{\mu \in \mathcal{P}_2(\mathbb{R}^d)} \mathcal{F}(\mu)$ (Ambrosio et al., 2008, Chapter 11).

3.1.3. DISCRETISED WASSERSTEIN GRADIENT FLOWS

For practical purposes, it is once more necessary to discretise the gradient flow in (16). Several popular approaches exist, including the backward Euler discretisation, which corresponds to the minimising movement scheme (MMS) (Ambrosio et al., 2008, Definition 2.0.6) or Jordan-Kinderlehrer-Otto (JKO) scheme (Jordan et al., 1998). Another natural choice for discretising (16) is a forward Euler scheme, which yields the Wasserstein (sub)gradient descent algorithm (e.g., Guo et al., 2022)

$$\mu_{t+1} = (\text{id} - \gamma \xi_t)_\# \mu_t, \quad \xi_t \in \partial \mathcal{F}(\mu_t). \quad (17)$$

For different choices of the functional \mathcal{F} , this discretisation yields the population limit of several existing particle-based algorithms. These include MMD gradient descent (Arbel et al., 2019), KSDD (Korba et al., 2021), and, replacing the Wasserstein gradient (17) by a kernel approximation, SVGD (Liu & Wang, 2016) and LAWGD (Chewi et al., 2020).

Regardless of the choice of numerical discretisation, the properties of the resulting algorithm depend, necessarily, on the choice of learning rate $\gamma > 0$. To illustrate this point, we recall the following bound for the Wasserstein subgradient descent algorithm (Guo et al., 2022, Theorem 8)

$$\mathcal{F}\left(\frac{1}{T} \sum_{t=1}^T \mu_t\right) - \mathcal{F}(\pi) \leq \frac{1}{T} \left[\frac{W_2^2(\mu_1, \pi)}{2\gamma} + \frac{L^2 T \gamma}{2} \right], \quad (18)$$

which holds under the assumption that the Wasserstein subgradients $\|\xi_t\|_{L^2(\mu_t)} \leq L$. We note that a similar bound also holds for the Langevin Monte Carlo (LMC) algorithm (Durmus et al., 2019, Section 3).

Based on (18), the optimal worst case learning rate is given by $\gamma_{\text{ideal}} = \frac{W_2^2(\mu_1, \pi)}{L\sqrt{T}}$, and thus the optimal error bound as

$$\mathcal{F}\left(\frac{1}{T} \sum_{t=1}^T \mu_t\right) - \mathcal{F}(\pi) \leq \frac{LW_2(\mu_1, \pi)}{\sqrt{T}}. \quad (19)$$

Similar to the Euclidean case, however, this rate cannot be achieved in practice. In particular, computing γ_{ideal} now depends on the unknown Wasserstein distance $W_2(\mu_1, \pi)$.

3.2. Coin Wasserstein Gradient Descent

We now introduce an alternative approach to solving the optimisation problem in (15), which is entirely learning rate free. Consider an infinite set of gamblers, indexed by $x_0 \in \mathbb{R}^d$. We will assume that the gamblers have initial wealth $w_0 := w_0(x_0)$, where $w_0 : \mathbb{R}^d \rightarrow \mathbb{R}_{\geq \varepsilon}$, $\varepsilon > 0$. Similar to before, in the t^{th} round, each gambler bets $x_t(x_0) \in \mathbb{R}^d$ on the outcome $c_t(x_0) \in \mathbb{R}^d$, and earns $\langle x_t(x_0), c_t(x_0) \rangle$. Once again, we assume the bets satisfy $x_t(x_0) = \beta_t w_{t-1}(x_0)$, for some betting fraction $\beta_t(x_0) \in [-1, 1]^d$.

Importantly, will now view $x_t : \mathbb{R}^d \rightarrow \mathbb{R}^d$ as a function, which defines the bets associated with gambler $x_0 \in \mathbb{R}^d$. Similarly, $w_t : \mathbb{R}^d \rightarrow \mathbb{R}_{\geq \varepsilon}$, $c_t : \mathbb{R}^d \rightarrow \mathbb{R}^d$, and $\beta_t : \mathbb{R}^d \rightarrow [-1, 1]^d$ are now all to be viewed as functions. We also now introduce a betting distribution $\mu_t^x \in \mathcal{P}_2(\mathbb{R}^d)$, defined as the push-forward of some initial betting distribution, μ_0^x , under the betting function $x_t : \mathbb{R}^d \rightarrow \mathbb{R}^d$. This definition is quite natural. In particular, it implies that, for a gambler $x_0 \sim \mu_0^x$, the bet $x_t := x_t(x_0)$ made by this gambler are distributed according to the betting distribution μ_t^x .

To obtain the parameter-free Wasserstein gradient descent algorithm, we will assume that the outcomes observed by the gambler $x_0 \in \mathbb{R}^d$, are given by the normalised Wasserstein gradients $c_t(x_0) = -\frac{1}{L} \nabla_{W_2} \mathcal{F}(\mu_t)(x_t(x_0))$, where L is the constant defined in Assumption 3.2. We will also suppose that this gambler's betting fraction is $\beta_t(x_0) = \frac{1}{t} \sum_{s=1}^{t-1} c_s(x_0)$. This leads to Algorithm 1.

3.3. Main Results

We will establish convergence of Algorithm 1 under the following general assumptions, in addition to a technical assumption in Appendix B.

Assumption 3.1. The functional $\mathcal{F} : \mathcal{P}_2(\mathbb{R}^d) \rightarrow (-\infty, \infty]$ is (i) proper and lower semi-continuous, and (ii) geodesically convex.

Assumption 3.2. There exists $L > 0$ such that, for all $u \in \mathbb{R}^d$, $\|\nabla_{W_2} \mathcal{F}(\mu_t^x)(u)\| \leq L$.

Assumption 3.1(i) is a general technical condition satisfied in all relevant cases (e.g., Ambrosio et al., 2008, Section 10). Assumption 3.1(ii) is a standard condition used in the analysis of existing sampling algorithms such as LMC (Wibisono,

Algorithm 1 Coin Wasserstein Gradient Descent

Input: initial measure $\mu_0^x \in \mathcal{P}_2(\mathbb{R}^d)$, initial parameter $x_0 \sim \mu_0^x$ or $x_0 \in \mathbb{R}^d$, initial wealth function $w_0 : \mathbb{R}^d \rightarrow \mathbb{R}_{\geq \varepsilon}$ satisfying $w_0 \in L^2(\mu_0^x)$, functional $\mathcal{F} : \mathcal{P}_2(\mathbb{R}^d) \rightarrow (-\infty, \infty]$, constant L .

for $t = 1$ **to** T **do**

 Compute

$$x_t(x_0) = -\frac{\sum_{s=1}^{t-1} \nabla_{W_2} \mathcal{F}(\mu_s^x)(x_s(x_0))}{Lt} \left(w_0(x_0) - \sum_{s=1}^{t-1} \left\langle \frac{1}{L} \nabla_{W_2} \mathcal{F}(\mu_s^x)(x_s(x_0)), x_s(x_0) \right\rangle \right). \quad (20)$$

 Define $\mu_t^x = (x_t)_{\#} \mu_0^x$.

Output: μ_T^x or $\frac{1}{T} \sum_{t=1}^T \mu_t^x$.

2018; Durmus & Moulines, 2019).³ This assumptions holds if $\mathcal{F}(\mu) = \text{KL}(\mu|\pi)$, and the potential $U : \mathbb{R}^d \rightarrow \mathbb{R}$ is convex (Ambrosio et al., 2008, Section 9.4).

To our knowledge, Assumption 3.2 has also only explicitly appeared in the analysis of the Wasserstein subgradient descent algorithm in Guo et al. (2022). However, similar conditions have also been used to analyse the convergence of SVGD to its population limit (Liu et al., 2017, Theorem 3.2; Korba et al., 2020, Proposition 7). On the other hand, convergence rates for SVGD (in the infinite particle regime) can be established under boundedness assumptions for the kernel function and either the KSD of the algorithm iterates (Liu et al., 2017), the Stein Fisher information (Korba et al., 2020), or the Hessian of the potential (Salim et al., 2022; Shi et al., 2022).

Theorem 3.3. *Let Assumptions 3.1 - 3.2 and Assumption B.1 (see Appendix B) hold. Then*

$$\begin{aligned} \mathcal{F} \left(\frac{1}{T} \sum_{t=1}^T \mu_t^x \right) - \mathcal{F}(\pi) &\leq \frac{L}{T} \left[\int_{\mathbb{R}^d} w_0(x) \mu_0^x(dx) \right. \\ &\quad \left. + \int_{\mathbb{R}^d} \|x\| \sqrt{T \ln \left(1 + \frac{24K_1^2 T^2 \|x\|^2}{\varepsilon^2} \right)} \pi(dx) \right]. \end{aligned} \quad (21)$$

Proof. See Appendix B. \square

The proof of Theorem 3.3 closely follows the proof used to establish the convergence rate of the parameter-free optimisation algorithm in Orabona & Pal (2016). In our case, however, it is no longer evident how to convert a lower bound on the wealth into an upper bound on the regret (see Lemma 2.1). In Appendix B, we provide a technical condition (Assumption B.1) which allow us to obtain the rate in Theorem 3.3. It remains an interesting direction for future work to obtain more easily verifiable conditions under which this result still holds.

³We note that one can establish convergence rates for LMC under weaker conditions, such as the log-Sobolev inequality (LSI) or the Poincaré inequality (PI) (Vempala & Wibisono, 2019). Similarly, convergence of SVGD can be established using the Stein LSI (Duncan et al., 2019; Korba et al., 2020), Talagrand’s inequality (Salim et al., 2022; Shi et al., 2022), or the PI (Chewi et al., 2020).

3.4. Practical Implementation

In practice, we do not directly observe the vector fields $\nabla_{W_2} \mathcal{F}(\mu_t^x)$. Indeed, these quantities depend on knowledge of the measures μ_t^x , which typically we cannot compute in closed form. Following existing ParVIs, a standard approach is to approximate these quantities using a set of interacting particles. In particular, suppose we initialise $(x_0^i)_{i=1}^N \stackrel{\text{i.i.d.}}{\sim} \mu_0^x(dx)$, with empirical law $\mu_0^N = \frac{1}{N} \sum_{i=1}^N \delta_{x_0^i}$. We can then update the particles according to an empirical version of (20). This yields, after each iteration, particles $(x_t^i)_{i=1}^N$, with empirical distribution $\mu_t^{x,N} = \frac{1}{N} \sum_{i=1}^N \delta_{x_t^i}$.

This approach relies, crucially, on being able to compute, or approximate $\nabla_{W_2} \{\mathcal{F}(\mu_t^{x,N})\}_{t \in [0,T]}$, the Wasserstein gradients of \mathcal{F} evaluated at $\{\mu_t^{x,N}\}_{t \in [0,T]}$. Fortunately, a similar step is also central to existing particle-based sampling algorithms, including SVGD (Liu & Wang, 2016), KSDD (Korba et al., 2020), and LAWGD (Chewi et al., 2020). We can thus use existing methods to compute these terms. In fact, as outlined in Appendix C, we can obtain learning-rate free versions of SVGD (Section C.1), LAWGD (Section C.2), and KSDD (Section C.3). We refer to these algorithms as Coin SVGD, Coin LAWGD, and Coin KSD, respectively.

In principle, our approach also requires knowledge of a bound on the Wasserstein gradients (see Assumption 3.2). In practice, we will adaptively estimate this constant using a similar approach to the one outlined in Orabona & Tommasi (2017). We provide full details in Appendix D.

4. Numerical Results

In this section, we evaluate the numerical performance of Coin SVGD (Algorithm 2), Coin LAWGD (Algorithm 3), and Coin KSDD (Algorithm 4). In all cases, we implement the adaptive versions of these algorithms (see Appendix D). We use the RBF kernel $k(x, x') = \exp(-\frac{1}{h} \|x - x'\|_2^2)$, with bandwidth chosen using the median heuristic in Liu & Wang (2016). The code to reproduce all results will be available on GitHub [post-review](#). Additional implementation details and results are provided in Appendix E.

4.1. Toy Examples

We begin by illustrating the performance of Coin SVGD on a series of toy examples (see Appendix E.1 for details). In the interest of space, results for Coin LAWGD and Coin KSDD are deferred to Appendices E.2 and E.3.

In Figure 1 (see Section 1), we plot the sampling approximations generated by SVGD and Coin SVGD after 1000 iterations, using 20 particles. Encouragingly, Coin SVGD converges to the target distribution in all cases, even those which do not satisfy the assumptions of our theorem (e.g., convexity). In fact, further simulations indicate that the performance of Coin SVGD is competitive with the best performance of SVGD, when using the optimal but a priori unknown learning rate (see Figure 7 in Appendix E.1).

4.2. Bayesian Independent Component Analysis

We next consider a Bayesian independent component analysis (ICA) model (e.g., Comon, 1994). Suppose we observe $\mathbf{x} \in \mathbb{R}^p$. The task of ICA is to infer the ‘unmixing matrix’ $\mathbf{W} \in \mathbb{R}^{p \times p}$ such that $\mathbf{x} = \mathbf{W}^{-1}\mathbf{s}$, where $\mathbf{s} \in \mathbb{R}^p$ denote the latent independent sources. We will assume each component s_i has the same density: $s_i \sim p_s$. The log-likelihood of this model is then given by $\log p(\mathbf{x}|\mathbf{W}) = \log |\mathbf{W}| + \sum_{i=1}^p p_s([\mathbf{W}\mathbf{x}]_i)$. For the prior, we assume that the entries of \mathbf{W} are i.i.d., with law $\mathcal{N}(0, 1)$. The posterior is then $p(\mathbf{W}|\mathbf{x}) \propto p(\mathbf{x}|\mathbf{W})p(\mathbf{W})$, with

$$\nabla_{\mathbf{W}} \log p(\mathbf{W}|\mathbf{x}) = (\mathbf{W}^{-1})^T - \frac{p'_s(\mathbf{W}\mathbf{x})}{p_s(\mathbf{W}\mathbf{x})} \mathbf{x}^T - \mathbf{W} \quad (22)$$

where p_s is chosen such that $\frac{p'_s(\cdot)}{p_s(\cdot)} = \tanh(\cdot)$. We are interested in sampling from $p(\mathbf{W}|\mathbf{x})$. In our experiments, we generate 1000 samples of \mathbf{x} from the ICA model, for $p \in \{2, 4, 8, 16\}$. We use $N = 10$ particles, and repeat each experiment 50 times. To assess convergence, we compute the Amari distance (Amari et al., 1995) between the true \mathbf{W} and the estimates $\{\hat{\mathbf{W}}_i\}_{i=1}^{10}$ generated by each algorithm. We run SVGD for three learning rate: the optimal rate, tuned when $p = 2$, and a smaller and larger learning rate.

Our results are plotted in Figure 2. For $p = 2$, the performance of Coin SVGD is similar to the performance of SVGD with the optimal learning rate. For $p \in \{4, 8, 16\}$, the gap between the performance of Coin SVGD and SVGD increases. In particular, as we increase the dimension, Coin SVGD increasingly outperforms SVGD with the original optimal learning rate. In some sense, these results are unsurprising. The learning rate for SVGD was tuned with $p = 2$, and it should not necessarily perform well for $p \in \{4, 8, 16\}$. At the same time, these results illustrate the advantages of our algorithm: Coin SVGD requires no tuning, yet still performs robustly across all of these experiments.

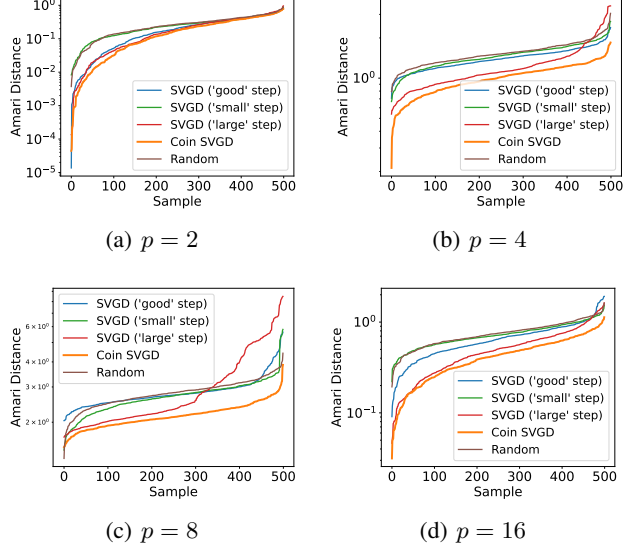


Figure 2. Results for the Bayesian ICA model: Amari distances between the true unmixing matrix and the estimated unmixing matrices output by SVGD and Coin SVGD (lower is better).

4.3. Bayesian Logistic Regression

We next consider the Bayesian logistic regression model for binary classification, as described in Gershman et al. (2012). Let $\mathcal{D} = \{\mathbf{x}_i, y_i\}_{i=1}^N$ be a dataset with feature vectors $\mathbf{x}_i \in \mathbb{R}^p$, and binary labels $y_i \in \{-1, 1\}$. We assume that $p(y_i = 1|\mathbf{x}_i, \mathbf{w}) = (1 + \exp(-\mathbf{w}^T \mathbf{x}_i))^{-1}$, for some $\mathbf{w} \in \mathbb{R}^p$. We place a Gaussian prior $p(\mathbf{w}|\alpha) = \mathcal{N}(\mathbf{w}|0, \alpha^{-1})$ on the regression weights \mathbf{w} , and a Gamma prior $p(\alpha) = \text{Gamma}(\alpha|1, 0.01)$ on $\alpha \in \mathbb{R}_+$.

We would like to sample from $p(\boldsymbol{\theta}|\mathcal{D})$, where the parameter of interest is given by $\boldsymbol{\theta} = [\mathbf{w}, \log \alpha]^T \in \mathbb{R}^{p+1}$. We test our algorithm using the Covertype dataset, which consists of 581,012 data points and 54 features. We randomly partition the data into a training dataset (70%), validation dataset (10%), and testing dataset (20%). We compute stochastic gradients using mini-batches of size 100.

Our results are plotted in Figures 3 and 4. Similar to before, the performance of Coin SVGD is similar to the best

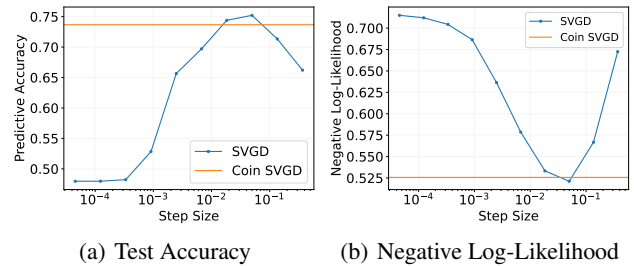


Figure 3. Results for the Bayesian logistic regression model: test-accuracy and the log-likelihood for SVGD and Coin SVGD.

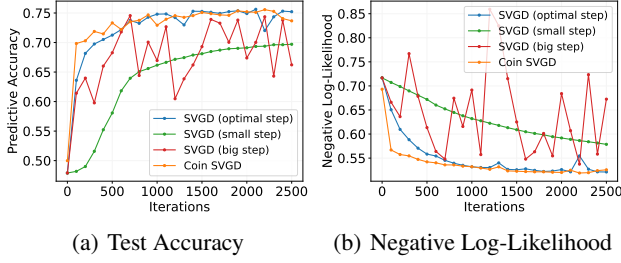


Figure 4. Results for the Bayesian logistic regression model: test-accuracy and the log-likelihood for SVGD (three learning rates) and Coin SVGD as a function of the number of iterations.

performance of SVGD. On the other hand, when the learning rate is too small or too large, Coin SVGD significantly outperforms SVGD.

4.4. Bayesian Neural Network

We next consider a Bayesian neural network model. Our settings are identical to those given in Liu & Wang (2016); see also (Hernandez-Lobato & Adams, 2015). In particular, we use a two-layer neural network with 50 hidden units with $\text{ReLU}(x) = \max(0, x)$ as the activation function. We assume the output is normal, and place a $\text{Gamma}(1, 0.1)$ prior on the inverse covariance. Meanwhile, we assign an isotropic Gaussian prior to the neural network weights.

In Figure 5, we plot the performance of our algorithm on 4 UCI datasets. In all cases, we randomly partition the data into 90% for training and 10% for testing. Our results indicate that SVGD typically outperforms Coin SVGD for well chosen learning rates, but significantly under-performs Coin SVGD when the learning rate is too small or too large. For certain datasets, the performance of Coin SVGD is very close to the optimal performance of SVGD, while for others, there remains a reasonable performance gap. This gap could be further reduced using recent advancements in parameter-free stochastic optimisation (e.g. Chen et al., 2022a;b).

4.5. Bayesian Probabilistic Matrix Factorisation

Finally, we consider a Bayesian probabilistic matrix factorisation (PMF) model (Salakhutdinov & Mnih, 2008). Let $\mathbf{R} \in \mathbb{R}^{N \times M}$ be a matrix of ratings for N users and M movies, where R_{ij} is the rating user i gave to movie j . Define matrices \mathbf{U} and \mathbf{V} for users and movies, respectively, where $\mathbf{U}_i \in \mathbb{R}^d$ and $\mathbf{V}_j \in \mathbb{R}^d$ are d -dimensional latent feature vectors for user i and movie j . The likelihood for the rating matrix is given by

$$p(\mathbf{R}|\mathbf{U}, \mathbf{V}, \alpha) = \prod_{i=1}^N \prod_{j=1}^M [\mathcal{N}(R_{ij}|\mathbf{U}_i^T \mathbf{V}_j, \alpha^{-1})]^{I_{ij}} \quad (23)$$

where I_{ij} denotes an indicator variable which equals 1 if users i gave rating for movie j . The priors for the users and

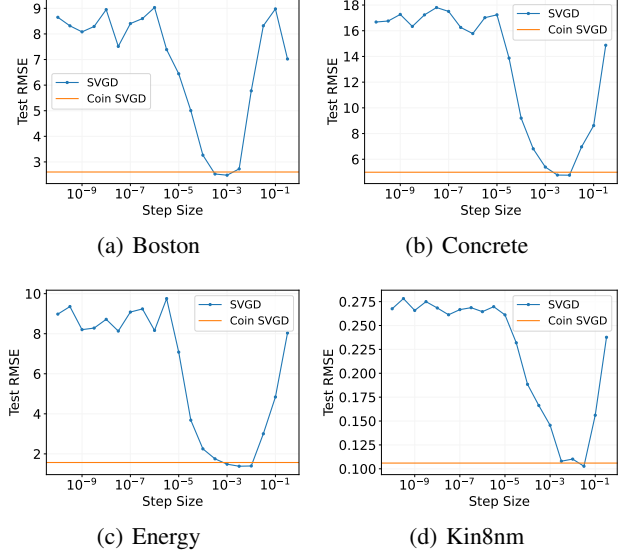


Figure 5. Results for the Bayesian neural network: test RMSE for SVGD and Coin SVGD after $T = 1000$ iterations for four UCI benchmark datasets.

movies are $p(\mathbf{U}|\mu_{\mathbf{U}}, \Lambda_{\mathbf{U}}) = \prod_{i=1}^N \mathcal{N}(\mathbf{U}_i|\mu_{\mathbf{U}}, \Lambda_{\mathbf{U}}^{-1})$ and $p(\mathbf{V}|\mu_{\mathbf{V}}, \Lambda_{\mathbf{V}}) = \prod_{j=1}^M \mathcal{N}(\mathbf{V}_j|\mu_{\mathbf{V}}, \Lambda_{\mathbf{V}}^{-1})$, with prior distributions on the hyper-parameters, for $\mathbf{W} = \mathbf{U}$ or \mathbf{V} , given by $\mu_{\mathbf{W}} \sim \mathcal{N}(\mu_{\mathbf{W}}|\mu_0, \Lambda_{\mathbf{W}})$ and $\Lambda_{\mathbf{W}} \sim \Gamma(a_0, b_0)$. The parameters of interest are then $\theta = (\mathbf{U}, \mu_{\mathbf{U}}, \Lambda_{\mathbf{U}}, \mathbf{V}, \mu_{\mathbf{V}}, \Lambda_{\mathbf{V}})$. In our experiments, we use hyper-parameters $(\alpha, \mu_0, a_0, b_0) = (3, 0, 4, 5)$, and set the latent dimension $d = 20$.

We test our algorithm on the MovieLens dataset (Harper & Konstan, 2015), which consists of 100,000 ratings, taking values $\{1, 2, 3, 4, 5\}$, for 1,682 movies from 943 users. The data are split into 80% for training and 20% for testing. We use $N = 10$ particles, and a batch size of 1000. We average our results over 5 random seeds.

Our results are shown in Figure 6, where we plot the root mean squared error (RMSE) for SVGD and Coin SVGD, as a function of the learning rate, after 1000 and 2000 iterations. We also compare against the stochastic gradient Langevin dynamics (SGLD) algorithm (Welling & Teh, 2011). In this case, Coin SVGD outperforms SVGD for almost all learning rates, and significantly outperforms SGLD.

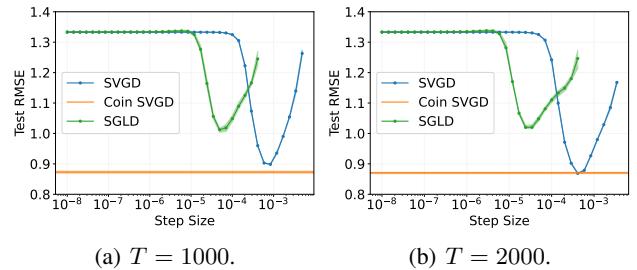


Figure 6. Results for the Bayesian probabilistic matrix factorisation model: RMSE for SGLD, SVGD, and Coin SVGD.

References

- Amari, S., Cichocki, A., and Yang, H. H. A New Learning Algorithm for Blind Signal Separation. In *Proceedings of the 8th International Conference on Neural Information Processing Systems (NIPS 1995)*, pp. 757–763, Denver, CO, 1995. doi: 10.5555/2998828.2998935.
- Ambrosio, L., Gigli, N., and Giuseppe Savaré. *Gradient Flows: In Metric Spaces and in the Space of Probability Measures*. Birkhäuser, Basel, 2008. ISBN 978-3-7643-8721-1. doi: 10.1007/978-3-7643-8722-8.
- Andrieu, C., de Freitas, N., Doucet, A., and Jordan, M. I. An Introduction to MCMC for Machine Learning. *Machine Learning*, 50(1):5–43, 2003. ISSN 1573-0565. doi: 10.1023/A:1020281327116.
- Arbel, M., Korba, A., Salim, A., and Gretton, A. Maximum Mean Discrepancy Gradient Flow. In *Proceedings of the 33rd International Conference on Neural Information Processing Systems (NeurIPS 2019)*, Vancouver, Canada, 2019.
- Bauschke, H. H. and Combettes, P. L. *Convex Analysis and Monotone Operator Theory in Hilbert Spaces*. Springer, New York, NY, 2011. doi: 10.1007/978-1-4419-9467-7.
- Brenier, Y. Polar factorization and monotone rearrangement of vector-valued functions. *Communications on Pure and Applied Mathematics*, 44(4):375–417, jun 1991. ISSN 0010-3640. doi: 10.1002/cpa.3160440402.
- Brézis, H. *Opérateurs maximaux monotones et semi-groupes de contractions dans les espaces de Hilbert*. Elsevier Science, Burlington, MA, 1973.
- Chen, C., Zhang, R., Wang, W., Li, B., and Chen, L. A Unified Particle Optimization Framework for Scalable Bayesian Sampling. In *Uncertainty in Artificial Intelligence*, Monterey, CA, 2018a.
- Chen, K., Cutkosky, A., and Orabona, F. Implicit Parameter-free Online Learning with Truncated Linear Models. In *Proceedings of the 33rd International Conference on Algorithmic Learning Theory (ALT 2022)*, Paris, France, 2022a.
- Chen, K., Langford, J., and Orabona, F. Better Parameter-Free Stochastic Optimization with ODE Updates for Coin Betting. In *Proceedings of the Thirty-Sixth AAAI Conference on Artificial Intelligence (AAAI-22)*, Online, 2022b.
- Chen, P. and Ghattas, O. Projected Stein Variational Gradient Descent. In *Proceedings of the 34th International Conference on Neural Information Processing Systems (NeurIPS 2020)*, Vancouver, Canada, 2020.
- Chen, W. Y., Mackey, L., Gorham, J., Briol, F.-X., and Oates, C. Stein Points. In *Proceedings of the 35th International Conference on Machine Learning (ICML 2018)*, Stockholm, Sweden, 2018b.
- Cheng, X. and Bartlett, P. Convergence of Langevin MCMC in KL-divergence. *Algorithmic Learning Theory*, pp. 186–211, 2018.
- Chewi, S., Le Gouic, T., Lu, C., Maunu, T., and Rigollet, P. SVGD as a kernelized Wasserstein gradient flow of the chi-squared divergence. In *Proceedings of the 34th International Conference on Neural Information Processing Systems (NeurIPS 2020)*, pp. 2098–2109, 2020.
- Chwialkowski, K., Strathmann, H., and Gretton, A. A Kernel Test of Goodness of Fit. In *Proceedings of the 33rd International Conference on Machine Learning (ICML 2016)*, New York, NY, 2016.
- Comon, P. Independent component analysis, A new concept? *Signal Processing*, 36(3):287–314, 1994. ISSN 0165-1684. doi: 10.1016/0165-1684(94)90029-9.
- Cutkosky, A. and Orabona, F. Black-Box Reductions for Parameter-free Online Learning in Banach Spaces. In *Proceedings of the 31st Annual Conference on Learning Theory (COLT 2018)*, Stockholm, Sweden, 2018.
- Dalalyan, A. S. Further and stronger analogy between sampling and optimization: Langevin Monte Carlo and gradient descent. In *Proceedings of the 30th Conference on Learning Theory (COLT 2017)*, Amsterdam, The Netherlands, 2017a.
- Dalalyan, A. S. Theoretical guarantees for approximate sampling from smooth and log-concave densities. *Journal of the Royal Statistical Society. Series B (Statistical Methodology)*, 79(3):651–676, sep 2017b. ISSN 13697412, 14679868.
- Dalalyan, A. S. and Karagulyan, A. User-friendly guarantees for the Langevin Monte Carlo with inaccurate gradient. *Stochastic Processes and their Applications*, 129(12):5278–5311, 2019. ISSN 0304-4149. doi: 10.1016/j.spa.2019.02.016.
- De Giorgi, E. New problems on minimizing movements. In *Boundary Value Problems for PDE and Applications*, pp. 81–98. Masson, Paris, 1993.
- Detommaso, G., Cui, T., Spantini, A., Marzouk, Y., and Scheichl, R. A Stein variational Newton method. In *Proceedings of the 32nd International Conference on Neural Information Processing Systems (NIPS 2018)*, Montreal, Canada, 2018.

- Duncan, A., Nusken, N., and Szpruch, L. On the geometry of Stein variational gradient descent. *arXiv preprint*, 2019. doi: 10.48550/arXiv.1912.00894.
- Durmus, A. and Moulines, É. Nonasymptotic convergence analysis for the unadjusted Langevin algorithm. *The Annals of Applied Probability*, 27(3):1551–1587, jun 2017. doi: 10.1214/16-AAP1238.
- Durmus, A. and Moulines, É. High-dimensional Bayesian inference via the unadjusted Langevin algorithm. *Bernoulli*, 25(4A):2854–2882, nov 2019. doi: 10.3150/18-BEJ1073.
- Durmus, A., Majewski, S., and Miasojedow, B. Analysis of Langevin Monte Carlo via Convex Optimization. *Journal of Machine Learning Research*, 20(1):2666–2711, 2019.
- Feng, Y., Wang, D., and Liu, Q. Learning to Draw Samples with Amortized Stein Variational Gradient Descent. In *Proceedings of the Conference on Uncertainty In Artificial Intelligence (UAI 2017)*, Sydney, Australia, 2017.
- Futami, F., Cui, Z., Sato, I., and Sugiyama, M. Frank-Wolfe Stein Sampling. *arXiv preprint*, 2019a. doi: 10.48550/arXiv.1805.07912.
- Futami, F., Cui, Z., Sato, I., and Sugiyama, M. Bayesian Posterior Approximation via Greedy Particle Optimization. In *Proceedings of the 33rd AAAI Conference on Artificial Intelligence*, Honolulu, HI, 2019b.
- Gelman, A., Carlin, J. B., Stern, H. S., Dunson, D. B., Vehtari, A., and Rubin, D. B. *Bayesian Data Analysis*. Chapman and Hall/CRC, New York, 3rd edition, 2013. doi: 10.1201/b16018.
- Gershman, S. J., Hoffman, M. D., and Blei, D. M. Nonparametric Variational Inference. In *Proceedings of the 29th International Conference on Machine Learning (ICML 2012)*, Edinburgh, UK, 2012.
- Gigli, N. On the inverse implication of Brenier-McCann theorems and the structure of $(P_2(M), W_2)$. *Methods and Applications of Analysis*, 18(2), 2011. doi: 10.4310/MAA.2011.v18.n2.a1.
- Gorham, J. and Mackey, L. Measuring Sample Quality with Kernels. In *Proceedings of the 34th International Conference on Machine Learning (ICML 2017)*, Sydney, Australia, 2017.
- Güler, O. On the Convergence of the Proximal Point Algorithm for Convex Minimization. *SIAM Journal on Control and Optimization*, 29(2):403–419, mar 1991. ISSN 0363-0129. doi: 10.1137/0329022.
- Guo, W., Hur, Y., Liang, T., and Ryan, C. T. Online Learning to Transport via the Minimal Selection Principle. In *Proceedings of the 35th Annual Conference on Learning Theory (COLT 2022)*, London, UK, 2022.
- Haario, H., Saksman, E., and Tamminen, J. Adaptive proposal distribution for random walk Metropolis algorithm. *Computational Statistics*, 14(3):375–395, 1999. ISSN 1613-9658. doi: 10.1007/s001800050022.
- Haarnoja, T., Tang, H., Abbeel, P., and Levine, S. Reinforcement Learning with Deep Energy-Based Policies. In *Proceedings of the 34th International Conference on Machine Learning (ICML 2017)*, Sydney, Australia, 2017.
- Han, J. and Liu, Q. Stein Variational Gradient Descent Without Gradient. In *Proceedings of the 35th International Conference on Machine Learning (ICML 2018)*, Stockholm, Sweden, 2018.
- Harper, F. M. and Konstan, J. A. The MovieLens Datasets: History and Context. *ACM Transactions on Interactive Intelligent Systems*, 5(4), 2015. ISSN 2160-6455. doi: 10.1145/2827872.
- Hartmann, M., Girolami, M., and Klami, A. Lagrangian Manifold Monte Carlo on Monge Patches. In *Proceedings of the 25th International Conference on Artificial Intelligence and Statistics (AISTATS 2022)*, Online, 2022.
- Hernandez-Lobato, J. M. and Adams, R. P. Probabilistic Backpropagation for Scalable Learning of Bayesian Neural Networks. In *Proceedings of the 32nd International Conference on Machine Learning (ICML 2015)*, Lille, France, 2015.
- Jordan, R., Kinderlehrer, D., and Otto, F. The Variational Formulation of the Fokker-Planck Equation. *SIAM Journal on Mathematical Analysis*, 29(1):1–17, 1998. doi: 10.1137/S0036141096303359.
- Jun, K.-S. and Orabona, F. Parameter-Free Online Convex Optimization with Sub-Exponential Noise. In *Proceedings of the 32nd Annual Conference on Learning Theory (COLT 2019)*, Phoenix, AZ, 2019.
- Korba, A., Salim, A., Arbel, M., Luise, G., and Gretton, A. A Non-Asymptotic Analysis for Stein Variational Gradient Descent. In *Proceedings of the 34th International Conference on Neural Information Processing Systems (NeurIPS 2020)*, Vancouver, Canada, 2020.
- Korba, A., Pierre-Cyril, Aubin-Frankowski, Majewski, S., and Ablin, P. Kernel Stein Discrepancy Descent. In *Proceedings of the 38th International Conference on Machine Learning (ICML 2021)*, Online, 2021.

- Krauth, W. *Statistical Mechanics: Algorithms and Computations*. Oxford University Press, 2006. ISBN 9780198515364.
- Krichevsky, R. and Trofimov, V. The performance of universal encoding. *IEEE Transactions on Information Theory*, 27(2):199–207, 1981. doi: 10.1109/TIT.1981.1056331.
- Leimkuhler, B. and Matthews, C. Efficient molecular dynamics using geodesic integration and solvent–solute splitting. *Proceedings of the Royal Society A: Mathematical, Physical and Engineering Sciences*, 472(2189): 20160138, may 2016. doi: 10.1098/rspa.2016.0138.
- Lelièvre, T. and Stoltz, G. Partial differential equations and stochastic methods in molecular dynamics. *Acta Numerica*, 25:681–880, 2016. ISSN 0962-4929. doi: DOI:10.1017/S0962492916000039.
- Li, L., Liu, Q., Korba, A., Yurochkin, M., and Solomon, J. Sampling with Mollified Interaction Energy Descent. *arXiv preprint*, 2022. doi: 10.48550/arXiv.2210.13400.
- Liu, C. and Zhu, J. Riemannian Stein Variational Gradient Descent for Bayesian Inference. In *Proceedings of the 32nd AAAI Conference on Artificial Intelligence*, New Orleans, LA, 2018.
- Liu, C., Zhuo, J., Cheng, P., Zhang, R., Zhu, J., and Carin, L. Understanding and Accelerating Particle-Based Variational Inference. In *Proceedings of the 36th International Conference on Machine Learning (ICML 2019)*, Long Beach, CA, 2019a.
- Liu, C., Zhuo, J., and Zhu, J. Understanding MCMC Dynamics as Flows on the Wasserstein Space. In *Proceedings of the 36th International Conference on Machine Learning (ICML 2019)*, Long Beach, CA, 2019b.
- Liu, D. C. and Nocedal, J. On the limited memory BFGS method for large scale optimization. *Mathematical Programming*, 45(1):503–528, 1989. ISSN 1436-4646. doi: 10.1007/BF01589116.
- Liu, J. S. *Monte Carlo Strategies in Scientific Computing*. Springer-Verlag, New York, 2009. ISBN 9780387763699.
- Liu, Q. Stein variational gradient descent as gradient flow. In *Proceedings of the 31st International Conference on Neural Information Processing Systems (NIPS 2017)*, pp. 3118–3126, Red Hook, NY, 2017. ISBN 9781510860964.
- Liu, Q. and Wang, D. Stein Variational Gradient Descent: A General Purpose Bayesian Inference Algorithm. In *Proceedings of the 30th Conference on Neural Information Processings Systems (NIPS 2016)*, Barcelona, Spain, 2016.
- Liu, Q., Lee, J. D., and Jordan, M. A Kernelized Stein Discrepancy for Goodness-of-fit Tests. In *Proceedings of the 33rd International Conference on Machine Learning (ICML 2016)*, New York, NY, 2016.
- Liu, X., Zhu, H., Ton, J.-F., Wynne, G., and Duncan, A. Grassmann Stein Variational Gradient Descent. In *Proceedings of the 25th International Conference on Artificial Intelligence and Statistics (AISTATS 2022)*, Online, 2022.
- Liu, Y., Ramachandran, P., Liu, Q., and Peng, J. Stein Variational Policy Gradient. In *Proceedings of the Conference on Uncertainty In Artificial Intelligence (UAI 2017)*, Sydney, Australia, 2017.
- Ma, Y.-A., Chen, T., and Fox, E. B. A complete recipe for stochastic gradient MCMC. In *Proceedings of the 28th International Conference on Neural Information Processing Systems (NIPS 2015)*, pp. 2917–2925, Montreal, Canada, 2015. doi: 10.5555/2969442.2969566.
- MacKay, D. J. *Information Theory, Inference, and Learning Algorithms*. Cambridge University Press, 2003. ISBN 9780521642989.
- Neal, R. M. *Bayesian Learning for Neural Networks*. Springer, New York, 1996. doi: 10.1007/978-1-4612-0745-0.
- Neal, R. M. Slice sampling. *The Annals of Statistics*, 31(3): 705–767, jun 2003. doi: 10.1214/aos/1056562461.
- Orabona, F. Simultaneous Model Selection and Optimization through Parameter-free Stochastic Learning. In *Proceedings of the 28th International Conference on Neural Information Processing Systems (NIPS 2014)*, Montreal, Canada, 2014.
- Orabona, F. A Modern Introduction to Online Learning. *arXiv preprint*, 2022. doi: 10.48550/arXiv.1912.13213.
- Orabona, F. and Cutkosky, A. Tutorial on Parameter-Free Online Learning. In *Proceedings of the 37th International Conference on Machine Learning (ICML 2020)*, Online, 2020.
- Orabona, F. and Pal, D. Coin Betting and Parameter-Free Online Learning. In *Proceedings of the 30th Conference on Neural Information Processings Systems (NIPS 2016)*, Barcelona, Spain, 2016.
- Orabona, F. and Tommasi, T. Training Deep Networks without Learning Rates Through Coin Betting. In *Proceedings of the 31st International Conference on Neural Information Processing Systems (NIPS 2017)*, Long Beach, CA, 2017.

- Otto, F. The Geometry of Dissipative Evolution Equations: The Porous Medium Equation. *Communications in Partial Differential Equations*, 26(1-2):101–174, jan 2001. ISSN 0360-5302. doi: 10.1081/PDE-100002243.
- Otto, F. and Westdickenberg, M. Eulerian Calculus for the Contraction in the Wasserstein Distance. *SIAM Journal on Mathematical Analysis*, 37(4):1227–1255, 2005. doi: 10.1137/050622420.
- Pagani, F., Wiegand, M., and Nadarajah, S. An n-dimensional Rosenbrock distribution for Markov chain Monte Carlo testing. *Scandinavian Journal of Statistics*, 49(2):657–680, jun 2022. ISSN 0303-6898. doi: 10.1111/sjos.12532.
- Peypouquet, J. and Sorin, S. Evolution Equations for Maximal Monotone Operators: Asymptotic Analysis in Continuous and Discrete Time. *Journal of Convex Analysis*, 17(3-4):1113–1163, 2010.
- Pu, Y., Gan, Z., Henao, R., Li, C., Han, S., and Carin, L. VAE Learning via Stein Variational Gradient Descent. In *Proceedings of the 31st International Conference on Neural Information Processing Systems (NIPS 2017)*, Long Beach, CA, 2017.
- Robert, C. P. and Casella, G. *Monte Carlo Statistical Methods*. Springer-Verlag, New York, 2 edition, 2004. doi: 10.1007/978-1-4757-4145-22.
- Salakhutdinov, R. and Mnih, A. Bayesian Probabilistic Matrix Factorization Using Markov Chain Monte Carlo. In *Proceedings of the 25th International Conference on Machine Learning (ICML 2008)*, pp. 880–887, New York, NY, 2008. ISBN 9781605582054. doi: 10.1145/1390156.1390267.
- Salim, A., Korba, A., and Luise, G. The Wasserstein Proximal Gradient Algorithm. In *Proceedings of the 34th International Conference on Neural Information Processing Systems (NeurIPS 2020)*, Vancouver, Canada, 2020.
- Salim, A., Sun, L., and Peter Richtárik. A Convergence Theory for SVGD in the Population Limit under Talagrand’s Inequality T1. In *Proceedings of the 39th International Conference on Machine Learning (ICML 2022)*, Online, 2022.
- Santambrogio, F. Euclidean, metric, and Wasserstein gradient flows: an overview. *Bulletin of Mathematical Sciences*, 7(1):87–154, 2017. ISSN 1664-3615. doi: 10.1007/s13373-017-0101-1.
- Shi, Y., Bortoli, V. D., Deligiannidis, G., and Doucet, A. Conditional Simulation Using Diffusion Schrödinger Bridges. In *Proceedings of the 10th International Conference on Learning Representations (ICLR 2022)*, Online, 2022.
- Shor, N. Z. *Minimization Methods for Non-Differentiable Functions*. Springer, Berlin, Heidelberg, 1985. doi: 10.1007/978-3-642-82118-9.
- Simon-Gabriel, C.-J. *Distribution-Dissimilarities in Machine Learning*. Phd, Eberhard Karls Universität Tübingen, Germany, 2018.
- Sun, L. and Richtárik, P. Improved Stein Variational Gradient Descent with Importance Weights. *arXiv preprint*, 2022. doi: 10.48550/arXiv.2210.00462.
- Vempala, S. S. and Wibisono, A. Rapid Convergence of the Unadjusted Langevin Algorithm: Isoperimetry Suffices. In *Proceedings of the 33rd International Conference on Neural Information Processing Systems (NeurIPS 2019)*, Vancouver, Canada, 2019.
- Villani, C. *Optimal Transport: Old and New*. Springer-Verlag, Berlin, 2008. ISBN 978-3-540-71049-3. doi: 10.1007/978-3-540-71050-9.
- Wang, D. and Liu, Q. Learning to Draw Samples: With Application to Amortized MLE for Generative Adversarial Learning. In *Proceedings of the 5th International Conference on Learning Representations (ICLR 2017)*, Toulon, France, 2017.
- Wang, D., Tang, Z., Bajaj, C., and Liu, Q. Stein Variational Gradient Descent with Matrix-Valued Kernels. In *Proceedings of the 33rd International Conference on Neural Information Processing Systems (NeurIPS 2019)*, Vancouver, Canada, 2019.
- Welling, M. and Teh, Y. W. Bayesian Learning via Stochastic Gradient Langevin Dynamics. In *Proceedings of the 28th International Conference on Machine Learning (ICML 2011)*, Bellevue, WA, 2011.
- Wenliang, L. K. and Kanagawa, H. Blindness of score-based methods to isolated components and mixing proportions. In *arXiv preprint*, 2021. doi: arXiv.2008.10087.
- Wibisono, A. Sampling as optimization in the space of measures: The Langevin dynamics as a composite optimization problem. In *Proceedings of the 31st Annual Conference on Learning Theory (COLT 2018)*, Stockholm, Sweden, 2018.
- Wilson, A. G. and Izmailov, P. Bayesian Deep Learning and a Probabilistic Perspective of Generalization. In *Proceedings of the 34th International Conference on Neural Information Processing Systems (NeurIPS 2020)*, Vancouver, Canada, 2020.
- Ye, M., Ren, T., and Liu, Q. Stein Self-Repulsive Dynamics: Benefits from Past Samples. In *Proceedings of the 34th International Conference on Neural Information Processing Systems (NeurIPS 2020)*, Vancouver, Canada, 2020.

- Yoon, J., Kim, T., Dia, O., Kim, S., Bengio, Y., and Ahn, S. Bayesian Model-Agnostic Meta-Learning. In *Proceedings of the 32nd International Conference on Neural Information Processing Systems (NIPS 2018)*, Montreal, Canada, 2018.
- Zhang, R., Chen, C., Li, C., and Carin, L. Policy Optimization as Wasserstein Gradient Flows. In *Proceedings of the 35th International Conference on Machine Learning (ICML 2018)*, Stockholm, Sweden, 2018.
- Zhu, Y. and Zabaras, N. Bayesian deep convolutional encoder–decoder networks for surrogate modeling and uncertainty quantification. *Journal of Computational Physics*, 366:415–447, 2018. ISSN 0021-9991. doi: 10.1016/j.jcp.2018.04.018.
- Zhuo, J., Liu, C., Shi, J., Zhu, J., Chen, N., and Zhang, B. Message Passing Stein Variational Gradient Descent. In *Proceedings of the 35th International Conference on Machine Learning (ICML 2018)*, Stockholm, Sweden, 2018.
- Zinkevich, M. Online Convex Programming and Generalized Infinitesimal Gradient Ascent. In *Proceedings of the 20th International Conference on Machine Learning (ICML 2003)*, ICML’03, pp. 928–935, Washington DC, 2003. AAAI Press. ISBN 1577351894. doi: 10.5555/3041838.3041955.

A. Background

A.1. Geodesic Convexity

In this section, we define a rigorous notion of convexity on the Wasserstein space. Let $\mu, \nu \in \mathcal{P}_2(\mathbb{R}^d)$. We define a constant speed geodesic between μ and ν as a curve $(\lambda_\eta^{\mu \rightarrow \nu})_{\eta \in [0,1]}$ such that $\lambda_0 = \mu$, $\lambda_1 = \nu$, and $W_2(\lambda_\iota, \lambda_\eta) = (\eta - \iota)W_2(\mu, \nu)$ for all $\iota, \eta \in [0, 1]$. If η_μ^ν is the optimal transport map between μ and ν , then a constant speed geodesic is given by

$$\lambda_\eta^{\mu \rightarrow \nu} = ((1 - \eta)\text{id} + \eta \mathbf{t}_\mu^\nu)_\# \mu. \quad (24)$$

Let $\mathcal{F} : \mathcal{P}_2(\mathbb{R}^d) \rightarrow (-\infty, \infty]$. The functional \mathcal{F} is said to be lower semi-continuous if, for all $M \in \mathbb{R}$, $\{\mathcal{F} \leq M\}$ is a closed subset of $\mathcal{P}_2(\mathbb{R}^d)$. For $m \geq 0$, we say that \mathcal{F} is m -geodesically convex if, for any $\mu, \nu \in \mathcal{P}_2(\mathbb{R}^d)$, there exists a constant speed geodesic $(\lambda_\eta^{\mu \rightarrow \nu})_{\eta \in [0,1]}$ between μ and ν such that, for all $\eta \in [0, 1]$,

$$\mathcal{F}(\lambda_\eta^{\mu \rightarrow \nu}) \leq (1 - \eta)\mathcal{F}(\mu) + \eta\mathcal{F}(\nu) - \frac{m}{2}\eta(1 - \eta)W_2^2(\mu, \nu). \quad (25)$$

In the case that this inequality holds for $m = 0$, we will simply say that \mathcal{F} is geodesically convex.

A.2. Subdifferential Calculus

We are now ready to introduce some basic concepts relating to subdifferential calculus in W_2 . This will provide us with the machinery to develop parameter-free methods for solving optimisation problems over $\mathcal{P}_2(\mathbb{R}^d)$. Let $\mu \in \mathcal{P}_2(\mathbb{R}^d)$, and let $\xi \in L^2(\mu)$. Let \mathcal{F} be a proper and lower semi-continuous functional on $\mathcal{P}_2(\mathbb{R}^d)$. We say that $\xi \in L^2(\mu)$ belongs to the Fréchet subdifferential of \mathcal{F} at μ , and write $\xi \in \partial\mathcal{F}(\mu)$ if, for any $\nu \in \mathcal{P}_2(\mathbb{R}^d)$,

$$\liminf_{\nu \rightarrow \mu} \frac{\mathcal{F}(\nu) - \mathcal{F}(\mu) - \int_{\mathbb{R}^d} \langle \xi(x), \mathbf{t}_\mu^\nu(x) - x \rangle \mu(dx)}{W_2(\nu, \mu)} \geq 0. \quad (26)$$

Suppose, in addition, that \mathcal{F} is m -geodesically convex. Then $\xi \in L^2(\mu)$ belongs to the Fréchet subdifferential $\partial\mathcal{F}(\mu)$ if and only if, for all $\nu \in \mathcal{P}_2(\mathbb{R}^d)$,

$$\mathcal{F}(\nu) - \mathcal{F}(\mu) \geq \int_{\mathbb{R}^d} \langle \xi(x), \mathbf{t}_\mu^\nu(x) - x \rangle \mu(dx) + \frac{m}{2}W_2^2(\mu, \nu). \quad (27)$$

For certain functionals \mathcal{F} , and under certain regularity conditions, (see Lemma 10.4.13 in [Ambrosio et al., 2008](#)), one has that $\partial\mathcal{F}(\mu) = \{\nabla_{W_2}\mathcal{F}(\mu)\}$, where $\nabla_{W_2}\mathcal{F}(\mu) \in L^2(\mu)$ is given by

$$\nabla_{W_2}\mathcal{F}(\mu) = \nabla \frac{\partial\mathcal{F}(\mu)}{\partial\mu}(x) \quad \text{for } \mu\text{-a.e. } x \in \mathbb{R}^d, \quad (28)$$

and $\frac{\partial\mathcal{F}(\mu)}{\partial\mu} : \mathbb{R}^d \rightarrow \mathbb{R}$ denotes the first variation of \mathcal{F} at μ , that is, the unique function such that

$$\lim_{\varepsilon \rightarrow 0} \frac{1}{\varepsilon} (\mathcal{F}(\mu + \varepsilon\zeta) - \mathcal{F}(\mu)) = \int_{\mathbb{R}^d} \frac{\partial\mathcal{F}(\mu)}{\partial\mu}(x) \zeta(dx), \quad (29)$$

where $\zeta = \nu - \mu$, and $\nu \in \mathcal{P}_2(\mathbb{R}^d)$. We will refer to $\nabla_{W_2}\mathcal{F}(\mu)$ as the Wasserstein gradient of \mathcal{F} at μ .

B. Theoretical Results

B.1. Lemma 2.1

Lemma 2.1. This result is well known; see, e.g., Lemma 1 in Orabona & Pal (2016); Theorem 9.6 in Orabona (2022); Section 4 in Orabona & Tommasi (2017); Part 2 in (Orabona & Cutkosky, 2020). In particular, we have

$$\begin{aligned}
 f\left(\frac{1}{T}\sum_{t=1}^T x_t\right) - f(x^*) &\leq \frac{1}{T}\sum_{t=1}^T \left(f(x_t) - f(x^*)\right) && \text{(Jensen's inequality)} \\
 &\leq \frac{1}{T}\left(\sum_{t=1}^T c_t x^* - \sum_{t=1}^T c_t x_t\right) && \text{(convexity)} \\
 &\leq \frac{1}{T}\left(\left(\sum_{t=1}^T c_t\right)x^* - h\left(\sum_{t=1}^T c_t\right) + \varepsilon\right) && \text{(definition of } h(\cdot)\text{)} \\
 &\leq \frac{1}{T}\left(\max_v [vx^* - h(v)] + \varepsilon\right) && \text{(maximum over } v = \sum_{t=1}^T c_t\text{)} \\
 &= \frac{h^*(x^*) + \varepsilon}{T}. && \text{(definition of } h^*(\cdot)\text{)}
 \end{aligned}$$

□

B.2. Theorem 3.3

In this section, we outline how to prove Theorem 3.3. This proof relies on a rather technical assumption, which we state below (Assumption B.1). The task of establishing more easily verifiable conditions under which this assumption holds remains an interesting direction for future work.

B.2.1. PROOF UNDER ASSUMPTION B.1

Assumption B.1. Let $x_t : \mathbb{R}^d \rightarrow \mathbb{R}^d$ and $\mu_t^x \in \mathcal{P}_2(\mathbb{R}^d)$ be defined as in Algorithm 1. For $t = 0, \dots, T$, let $t_{\mu_t^x}^\pi : \mathbb{R}^d \rightarrow \mathbb{R}^d$ and $t_{\pi}^{\mu_t^x} : \mathbb{R}^d \rightarrow \mathbb{R}^d$ denote the optimal transport maps from $\mu_t^x \mapsto \pi$ and from $\pi \mapsto \mu_t^x$, respectively. In addition, let $\tilde{t}_{\pi,t}^{\mu_t^x} := x_t \circ t_{\pi}^{\mu_t^x} : \mathbb{R}^d \rightarrow \mathbb{R}^d$ denote the transport map from π to μ_t^x , defined as the composition of x_t and $t_{\pi}^{\mu_t^x}$. Define the functions $v : \mathbb{R}^d \rightarrow \mathbb{R}^d$ and $\tilde{v} : \mathbb{R}^d \rightarrow \mathbb{R}^d$ according to

$$v(x) = \sum_{t=1}^T -\nabla_{W_2} \mathcal{F}(\mu_t^x)(t_{\pi}^{\mu_t^x}(x)), \quad \tilde{v}(x) = \sum_{t=1}^T -\nabla_{W_2} \mathcal{F}(\mu_t^x)(\tilde{t}_{\pi,t}^{\mu_t^x}(x)). \quad (30)$$

Then there exists a constant $K_1 > 0$ such that, for all $x \in \mathbb{R}^d$,

$$\frac{1}{4L^2T} [||v(x)||^2 - ||\tilde{v}(x)||^2] \leq \ln K_1. \quad (31)$$

Proof. Our proof begins in much the same fashion as the proof of Lemma 2.1. On this occasion, we consider

$$\mathcal{F}\left(\frac{1}{T}\sum_{t=1}^T \mu_t^x\right) - \mathcal{F}(\pi) \leq \frac{1}{T}\sum_{t=1}^T \mathcal{F}(\mu_t^x) - \mathcal{F}(\pi) \quad (32)$$

$$\leq \frac{1}{T}\sum_{t=1}^T \int_{\mathbb{R}^d} \langle -\nabla_{W_2} \mathcal{F}(\mu_t^x)(x), t_{\mu_t^x}^\pi(x) - x \rangle \mu_t^x(dx) \quad (33)$$

$$\leq \frac{L}{T} \int_{\mathbb{R}^d} \left\langle \sum_{t=1}^T -\nabla_{W_2} \hat{\mathcal{F}}(\mu_t^x)(t_{\pi}^{\mu_t^x}(x)), x \right\rangle \pi(dx) \quad (34)$$

$$- \frac{L}{T} \int_{\mathbb{R}^d} \sum_{t=1}^T \langle -\nabla_{W_2} \hat{\mathcal{F}}(\mu_t^x)(x_t(x)), x_t(x) \rangle \mu_0^x(dx)$$

where in the first line we have used Jensen's inequality, in the second line we have used the definition of geodesic convexity (see Section A), and in the third line we have substituted $x \mapsto t_{\pi^x}^{\mu_t^x}(x)$ and $x \mapsto x_t(x)$ in the first and second integrals, respectively, used the fact that $(t_{\pi^x}^{\mu_t^x})_{\#}\pi = \mu_t^x$ and $(x_t)_{\#}\mu_0^x = \mu_t^x$ (see Algorithm 1), and introduced the notation $\hat{\mathcal{F}} = \frac{1}{L}\mathcal{F}$.

By construction, the betting strategy in Algorithm 1 guarantees that, for any $x \in \mathbb{R}^d$, initial wealth function $w_0 : \mathbb{R}^d \rightarrow \mathbb{R}_{\geq \varepsilon}$, and for any arbitrary sequence $c_1(x), \dots, c_T(x) \in \mathbb{R}^d$, such that $\|c_t(x)\| \leq 1$, there exists an even, logarithmically convex function $h_x : \mathbb{R} \rightarrow \mathbb{R}_+$, the 'coin betting potential', such that the 'wealth' is lower bounded as (Orabona & Pal, 2016, Proof of Theorem 3, Appendix C)

$$w_T(x) = w_0(x) + \sum_{t=1}^T \langle c_t(x), x_t(x) \rangle \geq h_x \left(\left\| \sum_{t=1}^T c_t(x) \right\| \right), \quad (35)$$

where we include the subscript x in $h_x(\cdot)$ to emphasise that this function depends on the parameter x via the initial wealth $w_0(x)$. In particular, the betting strategy in Algorithm 1 guarantees that this inequality holds with (Orabona & Pal, 2016, Appendix F.1, Proof of Corollary 5)

$$h_x(u) = w_0(x) \frac{2^T \Gamma(1) \Gamma(\frac{T+1}{2} + \frac{u}{2}) \cdot \Gamma(\frac{T+1}{2} - \frac{u}{2})}{\Gamma^2(\frac{1}{2}) \Gamma(T+1)}. \quad (36)$$

Due to Lemma 16 in Orabona & Pal (2016), we also have that

$$h_x(u) \geq i_x(u) := \frac{w_0(x)}{K\sqrt{T}} \exp\left(\frac{u^2}{2T}\right), \quad (37)$$

where $K = e\sqrt{\pi}$ is a universal constant. We will apply the inequality in (35) for the sequence $c_t(x) = -\nabla_{W_2} \hat{\mathcal{F}}(\mu_t)(x_t(x))$. In particular, substituting this sequence into (35), and using also the inequality in (37), we have that

$$w_0(x) - \sum_{t=1}^T \left\langle -\nabla_{W_2} \hat{\mathcal{F}}(\mu_t)(x_t(x)), x_t(x) \right\rangle \geq -i_x \left(\left\| \sum_{t=1}^T -\nabla_{W_2} \hat{\mathcal{F}}(\mu_t)(x_t(x)) \right\| \right). \quad (38)$$

Suppose, for each $x \in \mathbb{R}^d$, we define the function $i_x : \mathbb{R}^d \rightarrow (-\infty, \infty]$ according to $I_x(u) = i_x(\|u\|)$. By substituting this definition into (38), and then substituting (38) into (32) - (34), we then have

$$\begin{aligned} \mathcal{F} \left(\frac{1}{T} \sum_{t=1}^T \mu_t^x \right) - \mathcal{F}(\pi) &\leq \frac{L}{T} \left[\sum_{t=1}^T \int_{\mathbb{R}^d} \left\langle -\nabla_{W_2} \hat{\mathcal{F}}(\mu_t^x)(t_{\pi^x}^{\mu_t^x}(x)), x \right\rangle \pi(dx) \right. \\ &\quad \left. - \int_{\mathbb{R}^d} I_x \left(\sum_{t=1}^T -\nabla_{W_2} \hat{\mathcal{F}}(\mu_t^x)(x_t(x)) \right) \mu_0^x(dx) + \int_{\mathbb{R}^d} w_0(x) \mu_0^x(dx) \right] \end{aligned} \quad (39)$$

$$\begin{aligned} &= \frac{L}{T} \left[\int_{\mathbb{R}^d} \left\langle \sum_{t=1}^T -\nabla_{W_2} \hat{\mathcal{F}}(\mu_t^x)(t_{\pi^x}^{\mu_t^x}(x)), x \right\rangle \pi(dx) \right. \\ &\quad \left. - \int_{\mathbb{R}^d} J_x \left(\sum_{t=1}^T -\nabla_{W_2} \hat{\mathcal{F}}(\mu_t^x)(\tilde{t}_{\pi^x}^{\mu_t^x}(x)) \right) \pi(dx) + \int_{\mathbb{R}^d} w_0(x) \mu_0^x(dx) \right], \end{aligned} \quad (40)$$

where, in the second line, we have substituted $x \mapsto t_{\pi^x}^{\mu_t^x}(x)$, used the definition of $\tilde{t}_{\pi^x}^{\mu_t^x}(\cdot)$, used the fact that $(t_{\pi^x}^{\mu_t^x})_{\#}\pi = \mu_0^x$, and defined the function $J_x : \mathbb{R}^d \rightarrow (-\infty, \infty]$ according to $J_x(u) = I_{t_{\pi^x}^{\mu_t^x}(x)}(u)$. Suppose we also now define

$$u(x) = \sum_{t=1}^T -\nabla_{W_2} \hat{\mathcal{F}}(\mu_t^x)(t_{\pi^x}^{\mu_t^x}(x)) \quad , \quad \tilde{u}(x) = \sum_{t=1}^T -\nabla_{W_2} \hat{\mathcal{F}}(\mu_t^x)(\tilde{t}_{\pi^x}^{\mu_t^x}(x)) \quad , \quad A = \frac{\int_{\mathbb{R}^d} J_x(\tilde{u}(x)) \pi(dx)}{\int_{\mathbb{R}^d} J_x(u(x)) \pi(dx)} \quad (41)$$

Using this notation, we can now rewrite the previous inequality as

$$\mathcal{F} \left(\frac{1}{T} \sum_{t=1}^T \mu_t^x \right) - \mathcal{F}(\pi) \leq \frac{L}{T} \left[\int_{\mathbb{R}^d} \langle u(x), x \rangle \pi(dx) - \int_{\mathbb{R}^d} J_x(\tilde{u}(x)) \pi(dx) + \int_{\mathbb{R}^d} w_0(x) \mu_0^x(dx) \right] \quad (42)$$

$$= \frac{L}{T} \left[\int_{\mathbb{R}^d} A \left(\langle u(x), \frac{x}{A} \rangle - J_x(u(x)) \right) \pi(dx) + \int_{\mathbb{R}^d} w_0(x) \mu_0^x(dx) \right]. \quad (43)$$

Let us fix $x \in \mathbb{R}^d$, and write $\theta = u(x)$, $F(\cdot) = J_x(\cdot)$, and $x^* = \frac{x}{A}$. Using this notation, for fixed $x \in \mathbb{R}^d$, we can rewrite the first integrand in (43) as

$$\left\langle u(x), \frac{x}{A} \right\rangle - J_x(u(x)) := \langle \theta, x^* \rangle - F(\theta). \quad (44)$$

Taking the supremum over $\theta \in \mathbb{R}^d$ and using the definition of the convex conjugate, we can easily upper bound this expression by

$$\langle \theta, x^* \rangle - F(\theta) \leq \sup_{\theta \in \mathbb{R}^d} (\langle \theta, x \rangle - F(\theta)) \leq F^*(x^*), \quad (45)$$

where, as elsewhere, F^* denotes the Fenchel conjugate of F . Returning to our previous notation, and using the fact that $x \in \mathbb{R}^d$ was chosen arbitrarily, we thus have that

$$\left\langle u(x), \frac{x}{A} \right\rangle - J_x(u(x)) \leq J_x^*\left(\frac{x}{A}\right), \quad \text{for all } x \in \mathbb{R}^d. \quad (46)$$

Substituting this expression into (42) - (43), it now follows straightforwardly that

$$\mathcal{F}\left(\frac{1}{T} \sum_{t=1}^T \mu_t^x\right) - \mathcal{F}(\pi) \leq \frac{L}{T} \left[\int_{\mathbb{R}^d} A J_x^*\left(\frac{x}{A}\right) \pi(\mathrm{d}x) + \int_{\mathbb{R}^d} w_0(x) \mu_0^x(\mathrm{d}x) \right] \quad (47)$$

$$= \frac{L}{T} \left[\int_{\mathbb{R}^d} A I_x^*\left(\frac{\|t_{\mu_0^x}^\pi(x)\|}{A}\right) \mu_0^x(\mathrm{d}x) + \int_{\mathbb{R}^d} w_0(x) \mu_0^x(\mathrm{d}x) \right] \quad (48)$$

$$= \frac{L}{T} \left[\int_{\mathbb{R}^d} A i_x^*\left(\frac{\|t_{\mu_0^x}^\pi(x)\|}{A}\right) \mu_0^x(\mathrm{d}x) + \int_{\mathbb{R}^d} w_0(x) \mu_0^x(\mathrm{d}x) \right], \quad (49)$$

where in the second line we have substituted $x \mapsto t_{\mu_0^x}^\pi(x)$, used the fact that $(t_{\mu_0^x}^\pi)_{\#} \mu_0^x = \pi$, and used the definition of I_x ; and, in the final line, we have used the fact that the Fenchel conjugate of $i_x(\|\cdot\|)$ is $i_x^*(\|\cdot\|)$ since i_x^* is an even function (Bauschke & Combettes, 2011, Example 13.7). Now, Lemma 18 of Orabona & Pal (2016) allows to bound this Fenchel conjugate as

$$i_x^*(u) \leq |u| \sqrt{T \ln \left(1 + \frac{24T^2 u^2}{w_0^2(x)} \right)} - \frac{w_0(x)}{K\sqrt{T}}. \quad (50)$$

Substituting this into our previous bound (49), we finally arrive at

$$\begin{aligned} \mathcal{F}\left(\frac{1}{T} \sum_{t=1}^T \mu_t^x\right) - \mathcal{F}(\pi) &\leq \frac{L}{T} \left[\int_{\mathbb{R}^d} \|t_{\mu_0^x}^\pi(x)\| \sqrt{T \ln \left(1 + \frac{24T^2 \|t_{\mu_0^x}^\pi(x)\|^2}{A^2 w_0^2(x)} \right)} \mu_0^x(\mathrm{d}x) + \int_{\mathbb{R}^d} w_0(x) \left(1 - \frac{A}{K\sqrt{T}} \right) \mu_0^x(\mathrm{d}x) \right] \\ &\leq \frac{L}{T} \left[\int_{\mathbb{R}^d} \|x\| \sqrt{T \ln \left(1 + \frac{24T^2 \|x\|^2}{A^2 \varepsilon^2} \right)} \pi(\mathrm{d}x) + \int_{\mathbb{R}^d} w_0(x) \mu_0^x(\mathrm{d}x) \right], \end{aligned} \quad (51)$$

where in the second line we have used our assumption on μ_0^x . It remains to bound the constant A from below, or, equivalently, the constant A^{-1} from above. The required bound will follow directly from our technical assumption. In particular, simplifying the definition given in (41), we have that

$$A^{-1} = \frac{\int_{\mathbb{R}^d} w_0(t_{\mu_0^x}^\pi(x)) \exp \left[\frac{\|v(x)\|^2}{2L^2T} \right] \pi(\mathrm{d}x)}{\int_{\mathbb{R}^d} w_0(t_{\mu_0^x}^\pi(x)) \exp \left[\frac{\|\tilde{v}(x)\|^2}{2L^2T} \right] \pi(\mathrm{d}x)} \leq \frac{\int_{\mathbb{R}^d} w_0(t_{\mu_0^x}^\pi(x)) \exp \left[\frac{\|v(x)\|^2}{2L^2T} \right] \pi(\mathrm{d}x)}{\int_{\mathbb{R}^d} \frac{1}{K_1} w_0(t_{\mu_0^x}^\pi(x)) \exp \left[\frac{\|v(x)\|^2}{2L^2T} \right] \pi(\mathrm{d}x)} = K_1, \quad (52)$$

where the second inequality follows from the bound in Assumption B.1. Substituting this into (51), we finally arrive at

$$\mathcal{F}\left(\frac{1}{T} \sum_{t=1}^T \mu_t^x\right) - \mathcal{F}(\pi) \leq \frac{L}{T} \left[\int_{\mathbb{R}^d} \|x\| \sqrt{T \ln \left(1 + \frac{24K_1^2 T^2 \|x\|^2}{\varepsilon^2} \right)} \pi(\mathrm{d}x) + \int_{\mathbb{R}^d} w_0(x) \mu_0^x(\mathrm{d}x) \right]. \quad (53)$$

□

C. Coin ParVI Algorithms

C.1. Coin Stein Variational Gradient Descent

Let $\mathcal{F}(\mu) = \text{KL}(\mu|\pi)$, with $\nabla_{W_2}\mathcal{F}(\mu) = \nabla \ln \frac{d\mu}{d\pi}$. Let $k : \mathbb{R}^d \times \mathbb{R}^d \rightarrow \mathbb{R}$ denote a positive semi-definite kernel, and \mathcal{H}_k denote the associated reproducing kernel Hilbert space (RKHS). In addition, define the integral operator $\mathcal{K}_{\mu,k} : L^2(\mu) \rightarrow \mathcal{H}_k$ according to $\mathcal{K}_{\mu,k}f(x) = \int_{\mathbb{R}^d} k(x, y)f(y)\mu(dy)$.

Following [Liu & Wang \(2016\)](#), suppose that we replace $\nabla_{W_2}\mathcal{F}(\mu)$ by $\mathcal{K}_{\mu,k}\nabla_{W_2}\mathcal{F}(\mu)$, its image under the integral operator $\mathcal{K}_{\mu,k}$. This essentially plays the role of the Wasserstein gradient in \mathcal{H}_k . Using integration by parts, and recalling that $\pi \propto e^{-U}$, one can show that $\mathcal{K}_{\mu,k}\nabla_{W_2}\mathcal{F}(\mu) = \mathbb{E}_{x \sim \mu} [k(\cdot, x)\nabla U(x) - \nabla_2 k(\cdot, x)]$ (e.g., [Duncan et al., 2019](#); [Korba et al., 2020](#); [Chewi et al., 2020](#)). It follows, in particular, that

$$\mathcal{K}_{\mu_t^N,k}\nabla_{W_2}\mathcal{F}(\mu_t^N)(x_t^i) = \frac{1}{N} \sum_{j=1}^N \left[k(x_t^i, x_t^j) \nabla U(x_t^j) - \nabla_2 k(x_t^i, x_t^j) \right]. \quad (54)$$

Substituting this expression into Algorithm 1, we arrive at a learning-rate free analogue of the SVGD algorithm ([Liu & Wang, 2016](#)). This algorithm is summarised in Algorithm 2.

We note that this algorithm is not entirely tuning free, since we are still required to specify a bandwidth for the kernel $k : \mathbb{R}^d \times \mathbb{R}^d \rightarrow \mathbb{R}$. However, in practice, this parameter can be tuned automatically using the median rule ([Liu & Wang, 2016](#)).

Algorithm 2 Coin Stein Variational Gradient Descent

Input: initial measure $\mu_0^x \in \mathcal{P}_2(\mathbb{R}^d)$, initial particles $x_0^1, \dots, x_0^N \sim \mu_0^x$, initial wealth function $w_0 : \mathbb{R}^d \rightarrow \mathbb{R}_{\geq \varepsilon}$, constant L .

for $t = 1$ **to** T **do**

for $i = 1$ **to** N **do**

 Compute

$$x_t^i = - \frac{\sum_{s=1}^{t-1} \sum_{j=1}^N [k(x_s^i, x_s^j) \nabla U(x_s^j) - \nabla_2 k(x_s^i, x_s^j)]}{LNt} \left(w_0(x_0^i) - \sum_{s=1}^{t-1} \left\langle \frac{1}{NL} \sum_{j=1}^N [k(x_s^i, x_s^j) \nabla U(x_s^j) - \nabla_2 k(x_s^i, x_s^j)], x_s^i \right\rangle \right). \quad (55)$$

 Define $\mu_t^{x,N} = \frac{1}{N} \sum_{i=1}^N \delta_{x_t^i}$.

Output: $\mu_T^{x,N}$ or $\frac{1}{T} \sum_{t=1}^T \mu_t^{x,N}$.

C.2. Coin Laplacian Adjusted Wasserstein Gradient Descent

Let $\mathcal{F}(\mu) = \text{KL}(\mu|\pi)$, with $\nabla_{W_2}\mathcal{F}(\mu) = \nabla \ln \frac{d\mu}{d\pi}$. Following [Chewi et al. \(2020\)](#), suppose that we replace $\nabla_{W_2}\mathcal{F}(\mu)$ by $\nabla \mathcal{K}_{\pi,k_{\mathcal{L}}} \frac{d\mu}{d\pi}$, the gradient of the image of $\frac{d\mu}{d\pi}$ under the integral operator $\mathcal{K}_{\mu,k_{\mathcal{L}}}$. The kernel $k_{\mathcal{L}}$ is chosen such that $\mathcal{K}_{\pi,k_{\mathcal{L}}} = -\mathcal{L}_{\pi}^{-1}$, where \mathcal{L}_{π} denotes the infinitesimal generator of the overdamped Langevin diffusion with stationary distribution π .

In this case, we have that $\nabla \mathcal{K}_{\pi,k_{\mathcal{L}}} \frac{d\mu}{d\pi} = \mathbb{E}_{x \sim \mu} [\nabla_1 k_{\mathcal{L}}(\cdot, x)]$, and thus

$$\nabla \mathcal{K}_{\pi,k_{\mathcal{L}}} \frac{d\mu^N}{d\pi}(x_t^i) = \frac{1}{N} \sum_{j=1}^N \nabla_1 k_{\mathcal{L}}(x_t^i, x_t^j). \quad (56)$$

By using these gradients in Algorithm 1, we obtain a learning-rate free analogue of the LAWGD algorithm ([Chewi et al., 2020](#)). This algorithm is summarised in Algorithm 3.

Algorithm 3 Coin Laplacian Adjusted Wasserstein Gradient Descent

Input: initial measure $\mu_0^x \in \mathcal{P}_2(\mathbb{R}^d)$, initial particles $x_0^1, \dots, x_0^N \sim \mu_0^x$, initial wealth function $w_0 : \mathbb{R}^d \rightarrow \mathbb{R}_{\geq \varepsilon}$, constant L .

for $t = 1$ **to** T **do**

for $i = 1$ **to** N **do**

 Compute

$$x_t^i = - \frac{\sum_{s=1}^{t-1} \sum_{j=1}^N \nabla_1 k_{\mathcal{L}}(x_s^i, x_s^j)}{LNt} \left(w_0(x_0^i) - \sum_{s=1}^{t-1} \left\langle \frac{1}{NL} \sum_{j=1}^N \nabla_1 k_{\mathcal{L}}(x_s^i, x_s^j), x_s^i \right\rangle \right). \quad (57)$$

 Define $\mu_t^N = \frac{1}{N} \sum_{i=1}^N \delta_{x_t^i}$.

Output: $\mu_T^{x,N}$ or $\frac{1}{T} \sum_{t=1}^T \mu_t^{x,N}$.

C.3. Coin Kernel Stein Discrepancy Descent

Let $\mathcal{F}(\mu) = \frac{1}{2} \text{KSD}^2(\mu|\pi)$, where $\text{KSD}(\mu|\pi)$ is the kernel Stein discrepancy, defined according to (Liu et al., 2016; Chwialkowski et al., 2016; Gorham & Mackey, 2017)

$$\text{KSD}(\mu|\pi) = \sqrt{\int_{\mathbb{R}^d} \int_{\mathbb{R}^d} k_{\pi}(x, y) \mu(\mathrm{d}x) \mu(\mathrm{d}y)}, \quad (58)$$

and where k_{π} is the Stein kernel, defined in terms of the score $s = \nabla \log \pi$, and a positive semi-definite kernel k , as

$$k_{\pi}(x, y) = s^T(x) s(y) k(x, y) + s^T(x) \nabla_2 k(x, y) + \nabla_1 k^T(x, y) s(y) + \nabla_{\cdot 1} \nabla_2 k(x, y) \quad (59)$$

In this case, given a discrete measure $\mu^N = \frac{1}{N} \sum_{j=1}^N \delta_{x^j}$, the loss function and its gradient are given by

$$\mathcal{F}(\mu^N) = \frac{1}{N^2} \sum_{i,j=1}^N k_{\pi}(x^i, x^j) \quad , \quad \nabla_{x_i} \mathcal{F}(\mu_t^N) = \frac{1}{N^2} \sum_{j=1}^N \nabla_2 k_{\pi}(x_t^j, x_t^i). \quad (60)$$

By substituting these gradients into Algorithm 1, we obtain a learning-rate free analogue of KSDD (Korba et al., 2021).⁴ This algorithm is summarised in Algorithm 4.

Algorithm 4 Coin Kernel Stein Discrepancy Descent

Input: initial measure $\mu_0^x \in \mathcal{P}_2(\mathbb{R}^d)$, initial particles $x_0^1, \dots, x_0^N \sim \mu_0^x$, initial wealth function $w_0 : \mathbb{R}^d \rightarrow \mathbb{R}_{\geq \varepsilon}$, constant L .

for $t = 1$ **to** T **do**

for $i = 1$ **to** N **do**

 Compute

$$x_t^i = - \frac{\sum_{s=1}^{t-1} \sum_{j=1}^N \nabla_2 k_{\pi}(x_s^j, x_s^i)}{LN^2t} \left(w_0(x_0^i) - \sum_{s=1}^{t-1} \left\langle \frac{1}{N^2L} \sum_{j=1}^N \nabla_2 k_{\pi}(x_s^j, x_s^i), x_s^i \right\rangle \right). \quad (61)$$

 Define $\mu_t^{x,N} = \frac{1}{N} \sum_{i=1}^N \delta_{x_t^i}$.

Output: $\mu_T^{x,N}$ or $\frac{1}{T} \sum_{t=1}^T \mu_t^{x,N}$.

⁴In fact, Korba et al. (2021) also propose a learning-rate free version of KSDD based on the quasi-Newton L-BFGS algorithm (Liu & Nocedal, 1989). Our method provides an alternative approach based on the ‘coin-betting’ paradigm.

D. Coin Sampling with Adaptive Gradient Bounds

In principle, in order to implement Algorithm 1, one requires knowledge of a constant $L > 0$ such that, for all $u \in \mathbb{R}^d$, $\|\nabla_{W_2} \mathcal{F}(\mu_t^x)(u)\| \leq L$ for all $t = 1, \dots, T$. In practice, this constant may not be known a priori. In this case, following Orabona & Tommasi (2017), we can use a modified version of our algorithm in which the gradient bounds are adaptively estimated. This algorithm is summarised in Algorithm 5.

D.1. Adaptive Coin Wasserstein Gradient Descent

Algorithm 5 Adaptive Coin Wasserstein Gradient Descent

Input: initial measure $\mu_1^x \in \mathcal{P}_2(\mathbb{R}^d)$, initial parameter $x_1 \sim \mu_1^x$ or $x_1 \in \mathbb{R}^d$, functional $\mathcal{F} : \mathcal{P}_2(\mathbb{R}^d) \rightarrow (-\infty, \infty]$.

Initialise: for $j = 1, \dots, d$, $L_{0,j} = 0$, $G_{0,j} = 0$, $R_{0,j} = 0$.

for $t = 1$ **to** T **do**

 Compute the negative Wasserstein gradient: $c_t(x_1) = -\nabla_{W_2} \mathcal{F}(\mu_t^x)(x_t(x_1))$.

for $j = 1$ **to** d **do**

 Update the maximum observed scale $L_{t,j} = \max(L_{t-1,j}, |c_{t,j}(x_1)|)$.

 Update the sum of the absolute value of the gradients: $G_{t,j} = G_{t-1,j} + |c_{t,j}|$.

 Update the reward: $R_{t,j}(x_1) = \max(R_{t-1,j}(x_1) + c_{t,j}(x_1)(x_{t,j}(x_1) - x_{1,j}), 0)$

 Update the parameter

$$x_{t+1,j}(x_1) = x_{1,j} + \frac{\sum_{s=1}^t c_{s,j}(x_1)}{L_{t,j}(G_{t,j} + L_{t,j})} (L_{t,j} + n_{t,j}(x_1)). \quad (62)$$

 Define $\mu_{t+1}^x = (x_{t+1})_{\#} \mu_1^x$.

Output: μ_T^x .

D.2. Adaptive Coin Stein Variational Gradient Descent

We now provide the adaptive version of Coin SVGD (Algorithm 2). In the interest of brevity, we do not provide the adaptive versions of Coin LAWGD (Algorithm 3) and Coin KSDD (Algorithm 4). However, these are easily obtained by substituting the relevant gradients into the adaptive version of the Coin SVGD

Algorithm 6 Adaptive Coin Stein Variational Gradient Descent

Input: initial measure $\mu_1^x \in \mathcal{P}_2(\mathbb{R}^d)$; for $i = 1, \dots, N$, initial particles $x_1^1, \dots, x_1^N \stackrel{\text{i.i.d.}}{\sim} \mu_1^x$.

Initialise: for $i = 1, \dots, N$, $j = 1, \dots, d$, $L_{0,j}^i = 0$, $G_{0,j}^i = 0$, $R_{0,j}^i = 0$.

for $t = 1$ **to** T **do**

for $i = 1$ **to** N **do**

 Compute the negative gradient $c_t^i = -\frac{1}{N} \sum_{j=1}^N [k(x_t^i, x_t^j) \nabla U(x_t^j) - \nabla_2 k(x_t^i, x_t^j)]$.

for $j = 1$ **to** d **do**

 Update the maximum observed scale: $L_{t,j}^i = \max(L_{t-1,j}^i, |c_{t,j}^i|)$

 Update the sum of the absolute value of the gradients: $G_{t,j}^i = G_{t-1,j}^i + |c_{t,j}^i|$

 Update the reward $R_{t,j}^i = \max(R_{t-1,j}^i + \langle c_{t,j}^i, x_{t,j}^i - x_{1,j}^i \rangle, 0)$

 Update the parameter

$$x_{t+1,j}^i = x_{1,j}^i + \frac{\sum_{s=1}^t c_{s,j}^i}{L_{t,j}^i (G_{t,j}^i + L_{t,j}^i)} (L_{t,j}^i + R_{t,j}^i). \quad (63)$$

 Define $\mu_{t+1}^N = \frac{1}{N} \sum_{i=1}^N \delta_{x_t^i}$.

Output: μ_T^N .

Following Orabona & Tommasi (2017), when we use Algorithm 6 for the Bayesian neural network (see Section 4.4), the update equation becomes

$$x_{t+1,j}^i = x_{1,j}^i + \frac{\sum_{s=1}^t c_{s,j}^i}{L_{t,j}^i \max(G_{t,j}^i + L_{t,j}^i, \alpha L_{t,j}^i)} (L_{t,j}^i + R_{t,j}^i). \quad (64)$$

where $\alpha > 0$ is a positive constant which we set equal to 100.

E. Additional Experimental Results

E.1. SVGD vs Coin SVGD

We compare the performance of SVGD (Liu & Wang, 2016) and Coin SVGD (Algorithm 2) on the following two-dimensional distributions.

Two-Dimensional Gaussian. The first example is an anisotropic bivariate Gaussian distribution, viz

$$p(x) = \mathcal{N}(x|\mu, \Sigma) \quad (65)$$

where $\mu = (-1, 1)^\top$ and $\Sigma^{-1} = \begin{pmatrix} 3 & -0.5 \\ -0.5 & 1 \end{pmatrix}$.

Mixture of Two Two-Dimensional Gaussians. The next example is a mixture of two bivariate Gaussian distributions, with

$$p(x) = \alpha_1 \mathcal{N}(x; \mu_1, \Sigma_1) + \alpha_2 \mathcal{N}(x; \mu_2, \Sigma_2), \quad (66)$$

where $\alpha_1 = 0.5$, $\mu_1 = (-2, 2)^\top$, and $\Sigma_1 = \frac{1}{2}\mathbb{1}$; $\alpha_2 = 0.5$, $\mu_2 = (2, -2)^\top$, and $\Sigma_2 = \frac{1}{2}\mathbb{1}$.

Donut Distribution. For the next example, we consider an annulus or ‘donut’ distribution, with density

$$p(x) \propto \exp\left(-\frac{(|x| - r_0)^2}{2\sigma^2}\right) \quad (67)$$

where $r_0 = 2.5$ and $\sigma^2 = 0.5$.

Rosenbrock Distribution. We next consider the so-called Rosenbrock or ‘banana’ distribution (Pagani et al., 2022), a correlated two-dimensional distribution with density

$$p(x_1, x_2) \propto \exp\left[\left(\frac{x_1}{a} - \mu_1\right)^2 + (ax_2 + ab(x_1^2 + a^2) - \mu_2)^2\right],$$

with $a = -1$, $b = 1$, $\mu_1 = 0$, and $\mu_2 = 1$. This is a common example used to benchmark sampling algorithms (e.g., Haario et al., 1999; Ma et al., 2015; Ye et al., 2020).

Squiggle Distribution. Our next example is a two-dimensional ‘squiggle’ distribution; see, e.g., Appendix E in Hartmann et al. (2022). In this case, the target density is given by

$$p(x) \propto \exp\left[(x' - \mu)^T \Sigma^{-1} (x' - \mu)\right] \quad (68)$$

where $x'_1 = x_1$, $x'_2 = x_1 + \sin(\omega x_1)$; and $\mu = (1, 1)^\top$, $\Sigma = \begin{pmatrix} 2 & 0.25 \\ 0.25 & 0.5 \end{pmatrix}$, and $\omega = 2$.

Funnel Distribution. Our final example is a two-dimensional ‘funnel’ distribution, with density

$$p(x_1, x_2) \propto \mathcal{N}(x_1; \mu_1, \sigma_1^2) \mathcal{N}(x_2; \mu_2, \exp(\frac{x_1}{2})) \quad (69)$$

where $\mu_1 = 4$, $\mu_2 = 1$, and $\sigma_1^2 = 3$. This example, in ten-dimensions, was first introduced in (Neal, 2003) to illustrate the difficulty of sampling from some hierarchical models.

In Figure 7, we provide a more detailed comparison of the performance of SVGD and Coin SVGD, plotting the KSD for both algorithms after 1000 iterations as a function of the learning rate. Following Gorham & Mackey (2017), we use the inverse multi-quadratic (IMQ) kernel $k(x, x') = (c^2 + \|x - x'\|_2^2)^\beta$ to compute the KSD, where $c > 0$ and $\beta(-1, 0)$. We truncate each plot at approximately the largest value of the step size such that SVGD is numerically stable.

In most cases, with an optimally tuned step size, SVGD achieves the best performance, attaining the lowest value of the KSD. However, using a step size which is too small leads to very slow convergence, while using a step size which is too large leads to non-convergence and, ultimately, numerical instability. It is worth emphasising that it is difficult to determine a good step size, or to implement a line-search method, since SVGD does not minimise a simple function. On the other hand, Coin SVGD achieves performance close to, or even better than, the performance of optimally-tuned SVGD, without any need to tune a step size.

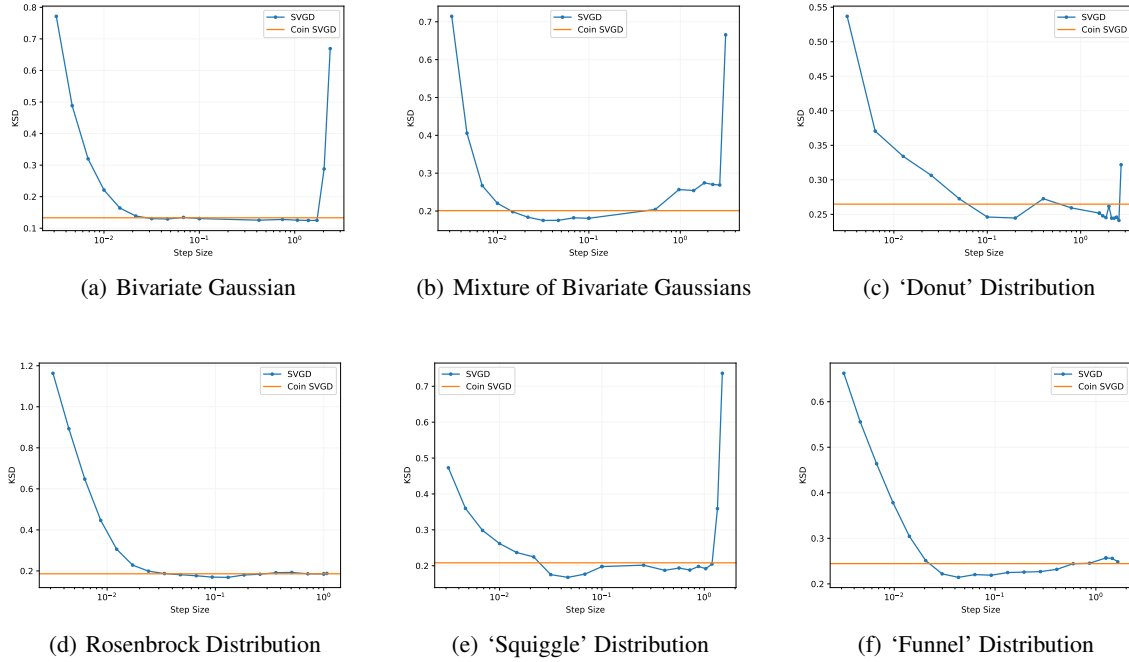


Figure 7. A comparison between SVGD (Liu & Wang, 2016) and its learning-rate free analogue, Coin SVGD (Algorithm 2). We plot the KSD of SVGD as a function of the step size, and the KSD of Coin SVGD, after $T = 1000$ iterations, for each of the two-dimensional target distributions plotted in Figure 1.

E.2. LAWGD vs Coin LAWGD

We now compare the performance of LAWGD (Chewi et al., 2020) and Coin LAWGD (Algorithm 3). In our two examples, we run the algorithm with $N = 100$ or $N = 25$ particles, and for $T = 2500$ iterations. Further details regarding implementation of LAWGD can be found in Chewi et al. (2020).

One-Dimensional Gaussian. We begin by considering a simple one-dimensional Gaussian, with density $p(x) = \mathcal{N}(x; \mu, \sigma^2)$, where $\mu = 3$ and $\sigma^2 = 1.5$.

Mixture of Three One-Dimensional Gaussians. We also consider a mixture of three one-dimensional Gaussians, with

$$p(x) = \sum_{i=1}^3 \alpha_i \mathcal{N}(x | \mu_i, \sigma_i^2), \quad (70)$$

where $\alpha_1 = \frac{1}{3}$, $\mu_1 = 6$, $\sigma_1^2 = 2$; $\alpha_2 = \frac{1}{2}$, $\mu_2 = -3$, and $\sigma_2^2 = 1$; and $\alpha_3 = \frac{1}{6}$, $\mu_3 = 2$, and $\sigma_3^2 = 1$.

It is worth noting that, even for relatively simple one- and two-dimensional examples, LAWGD is challenging to implement as it depends on spectral decomposition of a certain differential operator; see the discussion in Section 5 of Chewi et al. (2020). As a result, despite its attractive theoretical properties, LAWGD has not yet been widely adopted by practitioners. Nonetheless, we find it useful to include this comparison to demonstrate the flexibility of our coin-based methodology. Indeed, similar to before, we see that Coin LAWGD converges to the target distribution for both of our test cases, and enjoys a similar performance to the standard LAWGD algorithm (see Figure 8).

E.3. KSDD vs Coin KSDD

We next compare the performance of KSDD (Korba et al., 2021) and Coin KSDD (Algorithm 4). We use $N = 20$ particles; and run both methods for $T = 5000$ iterations. Similar to Korba et al. (2021), we consider the following toy-examples.

Anisotropic Two-Dimensional Gaussian. We first consider a single bivariate Gaussian, viz $p(x) = \mathcal{N}(x; \mu, \Sigma)$, where $\mu = (-3, 3)^\top$ and $\Sigma^{-1} = \begin{pmatrix} 0.2 & -0.05 \\ -0.05 & 0.1 \end{pmatrix}$.

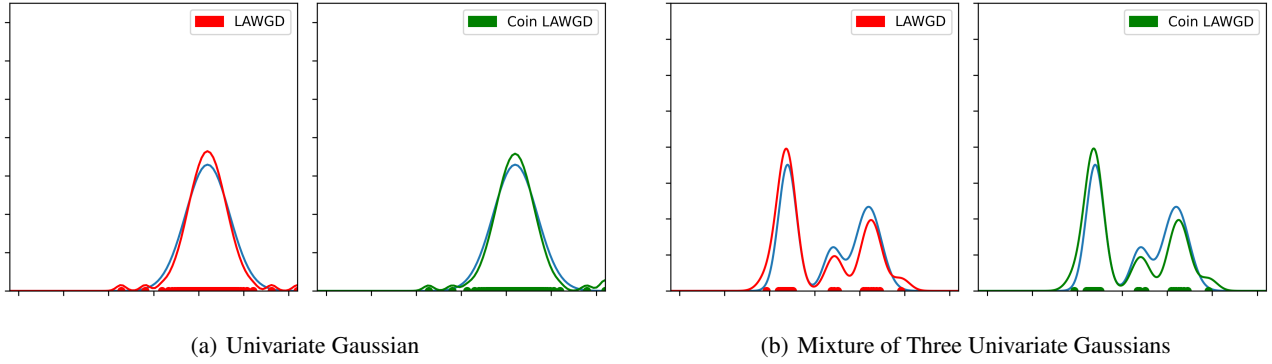


Figure 8. An illustrative comparison between LAWGD [Chewi et al. \(2020\)](#) and its learning-rate free analogue, Coin LAWGD ([Algorithm 3](#)). We plot the samples generated by both methods for the two target distributions detailed in [Section E.2](#).

Symmetric Mixture of Two Two-Dimensional Gaussians. In our second example, we consider a symmetric mixture of two, two-dimensional, isotropic Gaussians with the same variance: $p(x) = \frac{1}{2}\mathcal{N}(x; \mu, \sigma^2 \mathbb{1}) + \frac{1}{2}\mathcal{N}(x; -\mu, \sigma^2 \mathbb{1})$, where $\mu = (6, 0)^T$ and $\sigma^2 = 1$.

In [Figure 9](#), we plot the samples obtained using KSDD and Coin KSDD after 5000 iterations. Similar to before, the samples generated by the coin sampling method, step-size free algorithm are very similar to those generated by the original algorithm. In fact, even the dynamics of the two algorithms share many of the same properties. For example, the Coin KSDD particles seem initially to be guided by the final repulsive term in the update, which determine their global arrangement. They are then transported towards the mode(s), driven by the remaining score-based terms. This is in contrast to the Coin SVGD particles, which are first driven by the score term, before being dispersed around the mode by the repulsive term. These dynamics were first observed in [Korba et al. \(2021\)](#) for the standard SVGD and KSDD algorithms, and also to be present for their step-size free analogues.

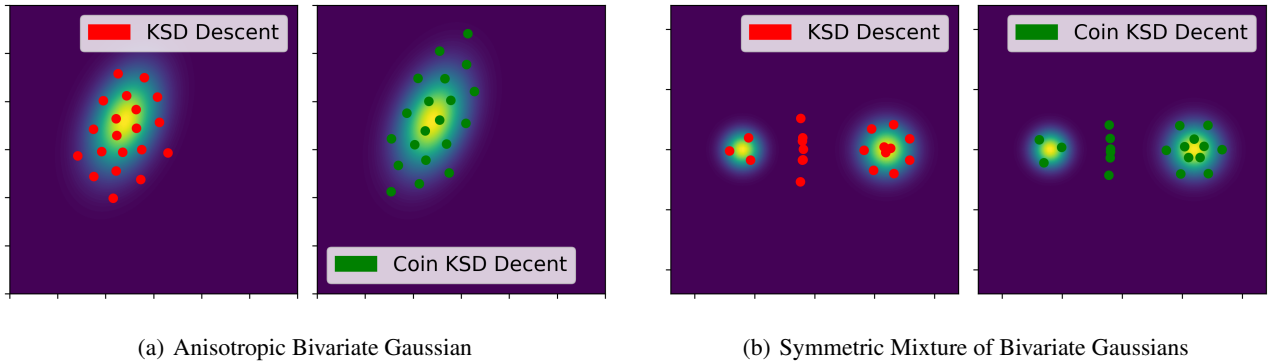


Figure 9. A comparison between KSDD ([Korba et al., 2021](#)) and its learning-rate free analogue, Coin KSDD ([Algorithm 4](#)). We plot the samples generated by both methods for the two target distributions detailed in [Section E.3](#).

Unsurprisingly, Coin KSDD also inherits some of the shortcomings of KSDD. Given a symmetric target, and a radial kernel, it is known that any plane of symmetry is invariant under the KSD gradient flow ([Korba et al., 2021](#), Lemma 11). Thus, if KSDD is initialised close to a plane of symmetry, it can become stuck there indefinitely. In practice, this also appears to hold true for Coin KSDD (see [Figure 9](#)). [Korba et al. \(2021\)](#) propose an annealing strategy can be used to resolve this behaviour; see also [Wenliang & Kanagawa \(2021\)](#). One first runs KSDD to obtain samples from the target $\pi_\beta(x) \propto \exp(-\beta U(x))$, where the inverse temperature $\beta \sim 0$. One then runs the algorithm a second time, initialised at these samples, on the true target $\pi(x) \propto \exp(-U(x))$. A similar strategy can also be used for Coin KSDD (see [Figure 10](#)).

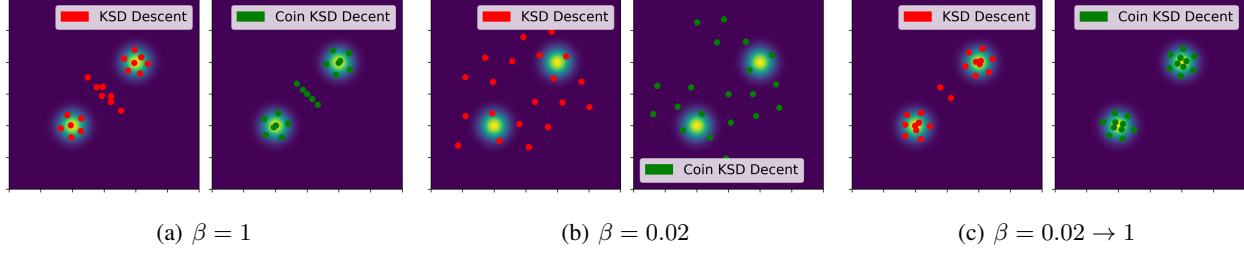


Figure 10. A comparison between annealing KSDD (Korba et al., 2021) and annealing Coin KSDD (Algorithm 4). We plot the samples generated by both methods using no annealing ($\beta = 1$), after the first step of the annealing method ($\beta = 0.02$), and after the full annealing method ($\beta = 0.02 \rightarrow \beta = 1$).

E.4. Bayesian Neural Network: Additional Numerical Results

Below we include additional results for the Bayesian neural network model. The experimental setting are all as described in Section 4.4,

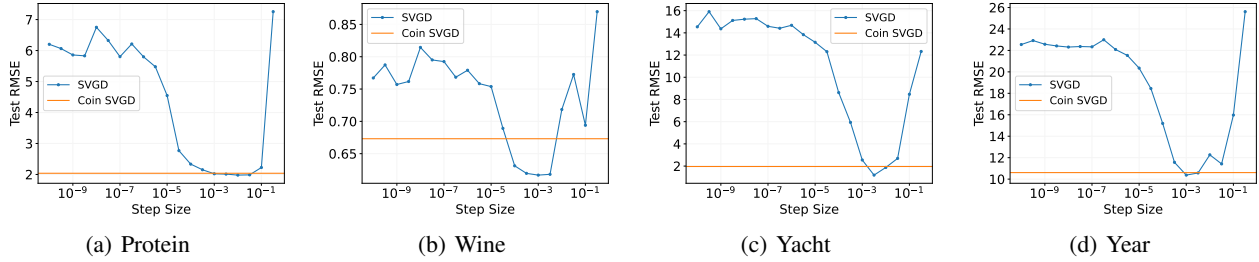


Figure 11. Results for the Bayesian neural network. We plot the test RMSE for SVGD and Coin SVGD for several UCI benchmark datasets. For each method, we use $N = 20$ particles and $T = 1000$ iterations.